3

Piezoelectric Resonators

Contributed by ARTHUR BALLATO

3.1 INTRODUCTION

This chapter provides a brief applications-oriented treatment of crystal resonators. Its objective is to make it possible for the user to specify the resonators best suited to the application from the standpoints of performance and cost. It aims also at helping the user to avoid the pitfalls of costly overspecification.

Piezoelectric resonators are circuit components that provide combinations of electrical parameters and other features such as temperature stability, not obtainable using conventional capacitors, inductors, and resistors. Physically, they consist of carefully oriented and dimensioned pieces of quartz crystal or other suitable piezoelectric material to which adherent electrodes have been applied. The crystals are held within sealed enclosures by mounting supports that also serve as connections between the electrodes and the external leads.

The electroded crystal forms a special kind of capacitor. Because it is piezoelectric, the crystal changes shape when a signal is applied to the electrodes. The amount of motion varies over wide extremes depending upon how closely the applied signal frequency approaches a natural mechanical resonance of the crystal. In a properly designed resonator these regions of high-amplitude mechanical vibration are very narrow in frequency and are ideally suited for oscillator stabilization. The piezoelectric effect is responsible for converting the electrical signal to mechanical motion and it reconverts the vibratory motion of the crystal back into an electrical signal at the resonator terminals. Looking at the resonator simply as a circuit component consisting of an enclosure and leads, it is not necessary to know what the enclosure contains. Its electrical behavior can be represented completely in network terms. This equivalent circuit is discussed in the next section.

The piezoelectric resonator is unique not only because of the achievable combinations of circuit parameter values but also because of other important features such as cost, size, and stability with time, temperature, and other environmental changes. To see how these factors affect performance we will occasionally look within the crystal enclosure in subsequent sections. In the present section we discuss general features of crystal resonators.

3.1.1 Frequency Range

Crystal resonators are available to cover frequencies from below 1 kHz to over 200 MHz. At the low-frequency end much current development is directed toward wristwatch applications at 32.768 kHz and powers of two times this frequency. This work has led to new families of miniature resonators (see Section 3.5). More conventional resonators span the range 80 kHz to 200 MHz; these utilize bulk acoustic waves (BAWs) that propagate within the crystal (see Sections 3.2 and 3.3). Recent work with BAW resonators has produced units at UHF frequencies (see Section 3.5). Surface acoustic waves (SAWs) travel along the crystal surface. Devices based on SAWs are becoming increasingly more available for the range above 50 MHz into the low GHz region (see Section 3.4).

3.1.2 Frequency Accuracy[3.20]

The absolute frequency accuracy of crystal-stabilized commercial oscillators has been improving at the rate of a factor of 10 every 20 years, starting around 1940 when the accuracy ranged between 10^{-3} and 10^{-4}. By 1980 the figure ranged from 10^{-5} to 10^{-6}, with 10^{-6} to 10^{-7} projected by 2000. These figures include total fractional absolute frequency variations over all environmental ranges such as temperature, mechanical shock, and aging.

3.1.3 Frequency Stability[3.20]

Precision quartz oscillators, held at constant temperature and protected from environmental disturbances, have shown improvement at the rate of a factor of 10 every 10 years. In 1960, fractional stabilities of 10^{-10}, 10^{-8}, and 10^{-6} had been achieved with laboratory versions, limited commercial production units, and in large-scale production, respectively. By 1980 these figures had improved to 10^{-12}, 10^{-10}, and 10^{-8}, with values of 10^{-14}, 10^{-12}, and 10^{-10} projected for the year 2000. These values are for observation times in the neighborhood of 0.1 to 10 s.

3.1.4 Enclosures

The great majority of crystal enclosures are designated by HC- numbers (Holder, Crystal). Two of the most popular sizes are shown in Figs. 3.1 and 3.2 to establish the general size range of resonators.

Holders are distinguished as follows:

1 Material: metal, glass, ceramic.
2 Terminals: pins, leads, tabs.
3 Method of sealing: solder, resistance weld, cold weld, thermocompression, induction heating.
4 Shapes and sizes: conventional metal cans, miniature tubes, glass envelopes, microcircuit (DIP) packages, transistor cans, ceramic flatpacks.

3.1.5 Crystal Vibrator (Bulk Wave Types)

The vibrator sealed within the enclosure is distinguished as follows:

1 Material: quartz, piezoelectric ceramic, high coupling single crystals such as lithium niobate or lithium tantalate.
2 Type of growth: natural or cultured (synthetic) quartz, other synthetic crystals hydrothermal or melt grown.
3 Treatment: as-grown (unswept), swept (electrolysis), etched.

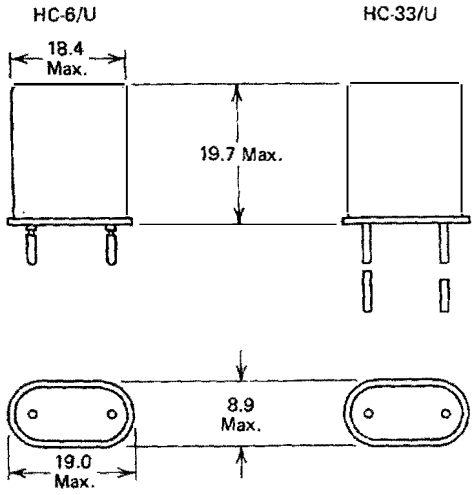

Figure 3.1 Standard crystal enclosures. Pin version HC-6/U, and wire lead version HC-33/U. Dimensions are in millimeters. Normally used for units in the frequency range 0.8 to 20 MHz.

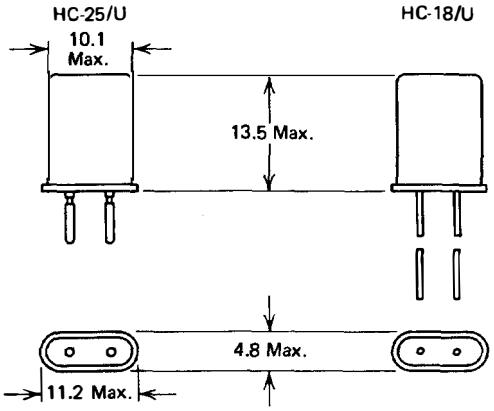

Figure 3.2 Standard crystal enclosures. Pin version HC-25/U and wire lead version HC-18/U. Dimensions are in millimeters. Normally used for units in the frequency range 10 to 200 MHz.

4 Crystal cut (orientation): unrotated, singly rotated, doubly rotated. Popular cuts are designated by names such as AT, BT, SC, and so on.

5 Vibrator geometry (plates, bars, forks, and so on) and dimensions.

6 Type of vibration: shear, extension, flexure, and so on. These may take place along one or more dimensions and may occur in combination.

7 Mode of vibration: what we have called the *type* of vibration is often called the *mode* of vibration. To avoid confusion we shall reserve the word *mode* to indicate one of the three polarizations of the vibrations that depend on the thickness dimension of a crystal plate. These are denoted the *a*, *b*, and *c* thickness modes, and are encountered in Section 3.3.

8 Overtone (harmonic) of operation.

9 Mounting supports: wire, strips, clamps, clips, and so on.

10 Crystal-to-mount bond: conductive bonding cement, epoxy, polymide; braze.

11 Electrode material: gold, aluminum, silver, copper; thin adhesion layer (Cr, Ti, Ni) plus gold.

12 Electrode deposition method: evaporation, sputtering, electroplating.

13 Ambient within enclosure: dry gas, for example, nitrogen, soft vacuum, high and ultrahigh vacuum.

These are discussed in greater detail in subsequent sections.

3.2 EQUIVALENT CIRCUITS

The symbol for a crystal resonator is shown in Fig. 3.3*a*. In precision applications, the metallic enclosure, leads and supports, and so on, require that

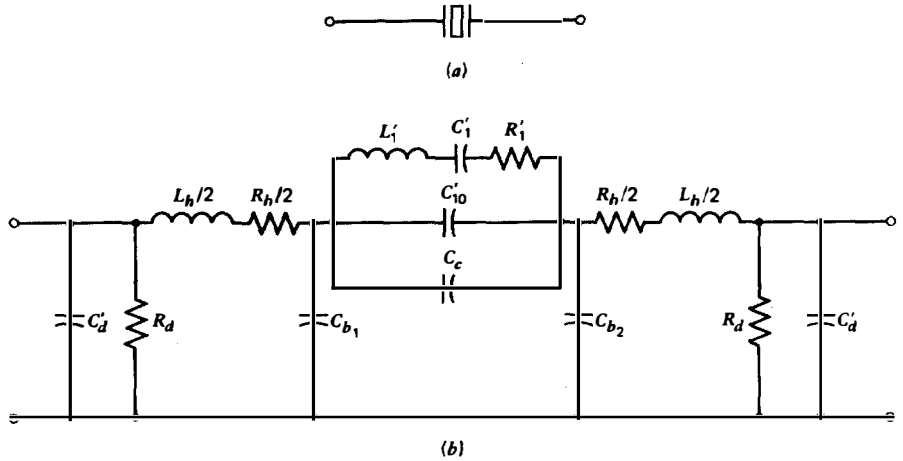

Figure 3.3 Crystal resonator. (a) Circuit symbol. (b) Complete equivalent circuit including the effects of holder and mounting supports. A single crystal resonance is represented by the L_1', C_1', R_1' arm. This circuit is valid in the vicinity of a single resonance up to UHF frequencies.

the resonator be treated as a two-port device. The complete circuit equivalent,[3.9] valid into the VHF range, is given in Fig. 3.3b and includes elements associated with the supports (R_h, L_h), enclosure and lead proximity (C_d', R_d), and electrode–enclosure capacitance (C_{b_1}, C_{b_2}, C_c). The crystal vibrator portion is represented in the vicinity of a single resonance by the C_{10}', C_1', R_1', and L_1' elements. It is virtually always the case that the influences of R_d and R_h can be neglected. Then, by suitable network manipulations, the complete circuit may be reduced to the circuit shown in Fig. 3.4, with the element values modified by the transformation.[3.9] The capacitors C_{d_1} and C_{d_2} range from a fraction of a picofarad to several picofarads; often they will be equal by manufacturing symmetry. Depending upon the method of utilizing the crystal, the presence of these capacitances will influence the resonator behavior. If the enclosure is metallic and is grounded to one lead, C_{10} is increased accordingly; if not, the shunt capacitors are lumped with the external circuit elements and have to be treated there. We are thus led to the four-element circuit of Fig. 3.5.[3.9, 3.10]

It is often the case that treatments of crystal resonator parameters end with a discussion of the R_1, L_1, C_1, and C_0 circuit seen at the enclosure terminals and an enumeration of these values. This is considered to be as far as the resonator designer has to go. Since these numbers completely characterize the resonator, it is reasoned, then any other needed quantities can be calculated. From the point of view of the designer of the circuit into which the resonator is to be placed, these same four quantities (or an equivalent set with L_1 replaced by the nominal resonance frequency) are likewise adequate to specify the crystal. A simple relation for the approximate frequency shift of the resonator when operated with series load capacitor C_L completes the crystal's portion of

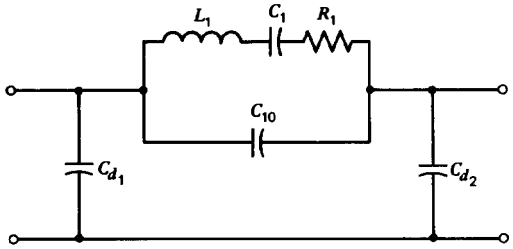

Figure 3.4 Equivalent electrical circuit of crystal resonator and enclosure. Below VHF frequencies the element values are constant; at higher frequencies the values are very weakly dependent on frequency, following from the constant values of Fig. 3.3*b*.

the design. Departures from the desired operating frequency and resonator power level are then corrected by mysterious time-consuming and costly "tweaking" procedures that result in nonoptimal designs.

In the systematic and straightforward procedures used in this book, somewhat more is asked of the resonator equivalent circuit, not the least of which is a reorientation of what is taken to be given in the resonator specification. Also required are more accurate expressions relating what is seen at the crystal terminals at the actual operating frequency; these are derived in the following sections.

Returning to Fig. 3.5, C_0 is called the *static* capacitance; it is the capacitance associated with the crystal and its adherent electrodes plus the stray capacitances internal to the crystal enclosure described above. It is a measured quantity that is specified. The value of C_0 does not include stray or wiring capacitance external to the enclosure. When these additional capacitances are added to C_0, the result is denoted as C_0'; this quantity is a specified value determined by the measured value of the latter effective stray capacitances added to C_0. The series R_1, L_1, C_1 portion is referred to as the *motional* arm of the circuit and arises from the mechanical crystal vibrations. C_1 and the resonator resistance R_L when operated with C_L in series, assuming $C_0' = C_0$ are both specified quantities. Also specified is df, a small frequency offset between the desired operating frequency, denoted simply as f, and the load frequency f_L obtained with C_L.

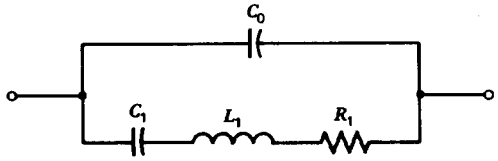

Figure 3.5 Simplified equivalent network of a crystal resonator. The element values are measured effective quantities that include various stray and parasitic effects, and are constant in the frequency regions centered about the resonance under consideration.

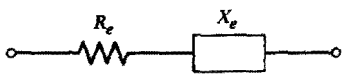

Figure 3.6 Resistive (R_e) and reactive (X_e) parts of the impedance represented by the network of Fig. 3.5. The quantities R_e and X_e are sensitive functions of frequency in the region of resonance.

3.2.1 R_e and X_e as Functions of Δf for the Case where $C_0' = C_0$

We assume that the presence of all stray capacitance internal to the enclosure has been resolved into the capacitor C_0, and that the resonator circuit plus internal strays remains of the form in Fig. 3.5. Expressions for the equivalent series resistance and reactance of the resonator are now derived using the $Z = R + \underline{X}$ representation covered in Section 1.2.1.5. Figure 3.6 is the network for the equivalent series resistance R_e and reactance X_e, which are functions of frequency.

The admittance of the network in Fig. 3.5 is

$$Y = \frac{1}{\underline{X}_0} + \frac{1}{R_1 + \underline{X}_1} = \frac{R_1 + \underline{X}_1 + \underline{X}_0}{\underline{X}_0(R_1 + \underline{X}_1)}. \tag{3.1}$$

The impedance $Z = Y^{-1}$ is then

$$Z = \frac{\underline{X}_0(R_1 + \underline{X}_1)}{R_1 + (\underline{X}_0 + \underline{X}_1)}. \tag{3.2}$$

Multiplication by $R_1 - (\underline{X}_0 + \underline{X}_1)$ gives

$$Z = R_e + \underline{X}_e = \frac{R_1^2\underline{X}_0 + R_1\underline{X}_0\underline{X}_1 - R_1\underline{X}_0(\underline{X}_1 + \underline{X}_0) - \underline{X}_1\underline{X}_0(\underline{X}_1 + \underline{X}_0)}{R_1^2 + (\underline{X}_1 + \underline{X}_0)^2}. \tag{3.3}$$

The real and imaginary parts of Eq. (3.3) are the series resistance R_e and series reactance X_e:

$$R_e = \frac{-R_1\underline{X}_0^2}{R_1^2 - (\underline{X}_1 + \underline{X}_0)^2} = \frac{R_1}{(R_1/X_0)^2 + ((X_0 + X_1)/X_0)^2}, \tag{3.4}$$

$$X_e = \frac{\underline{X}_0[R_1^2 - \underline{X}_1(\underline{X}_1 + \underline{X}_0)]}{R_1^2 - (\underline{X}_1 + \underline{X}_0)^2} = X_0\left\{\frac{R_1^2 + X_1(X_0 + X_1)}{R_1^2 + (X_0 + X_1)^2}\right\}. \tag{3.5}$$

These are sketched as functions of frequency over an extended range in Fig. 3.7. It is seen that X_e is zero at two values of frequency. The lower frequency is

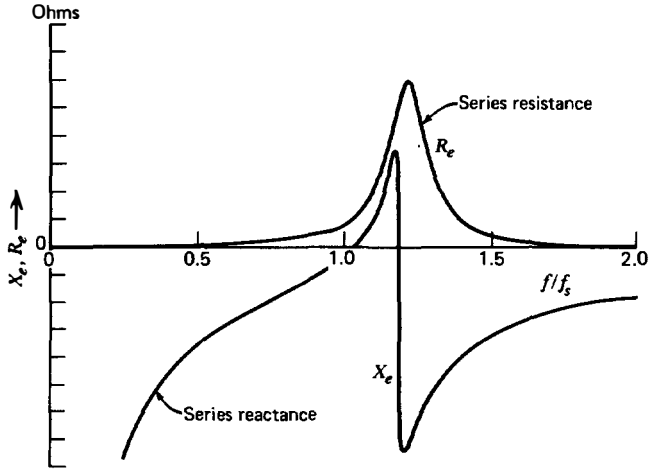

Figure 3.7 Resistive (R_e) and reactive (X_e) parts of the crystal resonator network of Fig. 3.5 as functions of frequency. X_e is zero at two frequencies; the lower one, denoted f_R, is the resonance frequency. At f_R, R_e is approximately R_1. Between the two zeros of X_e the resonator reactance appears inductive; the operating point of the resonator is normally somewhat above f_R.

just slightly above the series resonance frequency

$$f_s = \frac{1}{\left(2\pi\sqrt{L_1 C_1}\right.} \tag{3.6}$$

and is denoted the resonance frequency f_R. At f_R the equivalent resistance R_e is approximately R_1. The upper frequency at which X_e equals zero is usually denoted the antiresonance frequency f_A. At this point R_e is nearly a maximum. The high-impedance antiresonance frequency will not concern us further for oscillator applications.

With the assumption $|(X_0 + X_1)| \gg R_1$, Eqs. (3.4) and (3.5) become

$$R_e \approx \frac{R_1}{\quad} \tag{3.7}$$

$$X_e \approx \frac{X_1}{[(X_1 + X_0)/X_0]}. \tag{3.8}$$

These expressions are simplified further as follows:

Let $\omega = \omega_s + \Delta\omega$. Then $X_1 = \omega L_1 - 1/\omega C_1$ becomes

$$X_1 = \frac{1}{\omega C_1}\left(\frac{2\Delta\omega}{\omega_s} + \frac{\Delta\omega^2}{\omega_s^2}\right) \approx \frac{1}{\omega_s C_1}\left(\frac{2\Delta\omega}{\omega_s}\right) \tag{3.9}$$

or

$$X_1 \approx \frac{2}{\omega_s C_1}\frac{\Delta f}{f_s} \quad \text{assuming } \omega_s \gg \Delta\omega \tag{3.10}$$

Consistent with the approximations to follow and with the assumption that $\omega_s \gg \Delta\omega$, we will drop the subscript s and use $\Delta f/f$, where f is the actual operating frequency. Since $X_0 = -1/\omega C_0$, one obtains

$$\frac{X_1 + X_0}{X_0} \approx 1 - \frac{2C_0\Delta f}{C_1 f}. \tag{3.11}$$

Inserting Eq. (3.11) into Eqs. (3.7) and (3.8) gives

$$R_e \approx \frac{R_1}{(1 - 2C_0\Delta f/C_1 f)^2} \tag{3.12}$$

and

$$X_e \approx \frac{(2/\omega C_1)(\Delta f/f)}{(1 - 2C_0\Delta f/C_1 f)}. \tag{3.13}$$

Equation (3.13) may be further approximated by

$$X_e \approx \left(\frac{2}{\omega C_1}\right)\frac{\Delta f}{f}. \tag{3.13a}$$

The main assumption made in arriving at Eqs. (3.7) to (3.13) is that $|(X_0 + X_1)| \gg R_1$. This assumption is not universally valid. When $\Delta f = 0$, it is equivalent to the criterion

$$\frac{1}{\omega_s C_0 R_1} = M \gg 1. \tag{3.14}$$

The quantity M is one type of figure of merit and often is not large for overtone units (see Section 3.2.3.4). On the other hand, for any value of M, if $\Delta f \approx C_1 f/2C_0$, then $|X_0 + X_1| \approx 0$, and certainly is not $\gg R_1$. This frequency offset corresponds to the region of the antiresonance frequency, and by assumption is excluded from use.

3.2.2 R_e and X_e with Rated Load Capacitor C_L

The load capacitor C_L is a nonvariable specified quantity. Its presence in series with the resonator modifies R_e and X_e as follows: Assuming, as before, that $\Delta f/f \ll 1$, Eq. (3.10) gives an expression for X_1 in terms of Δf. This frequency

shift is now taken such that the positive reactance of X_1 equals the reactance magnitude of C_0 in parallel with C_L, so that the total reactance is zero:

$$\frac{2}{\omega_s C_1}\frac{\Delta f_{Ls}}{f} = \frac{1}{\omega(C_0 + C_L)} \tag{3.15}$$

or

$$\frac{(f_L - f_s)}{f} = \frac{\Delta f_{Ls}}{f} = \frac{C_1}{2(C_0 + C_L)} \tag{3.16}$$

Sometimes Δf_{Ls} and C_L are specified in place of C_1; Eq. (3.16) then determines C_1. Substitution of this value of $\Delta f/f$ in Eqs. (3.12) and (3.13) gives the values of $R_L = R_e$ and $X_L = X_e$ at the load frequency f_L:

$$R_L \approx R_1\left(\frac{C_0 + C_L}{C_L}\right)^2 \tag{3.17}$$

$$X_L \approx \frac{1}{\omega C_L} \tag{3.18}$$

As the load capacitance increases ($C_L^{-1} \to 0$), the load frequency f_L approaches the resonance frequency f_R, R_e approaches R_1, and X_L approaches zero.

In Fig. 3.8 the solid curves depict the variations of X_e and R_e in the vicinity of the operating point, wherein it is assumed that the static capacitance is the specified value C_0. The difference between f_s and f_R is exaggerated for clarity. At f_L the resistance is defined to be the load resistance R_L; its value is an input specification. In terms of the load resistance the quantity R_1 may be determined using Eq. (3.17):

$$R_1 = R_L\left(\frac{C_L}{C_0 + C_L}\right)^2 \tag{3.19}$$

An important derived quantity is the reactance change per change in fractional frequency. We denote this quantity as $\Delta X(\Delta f/f)^{-1}$ and calculate its value about the frequency f_s by using Eq. (3.13a). X_e equals zero at f_s, so the difference ΔX in reactance as the fractional frequency is changed by $\Delta f/f$ from this point is

$$\frac{\Delta X}{\Delta f/f} \approx \frac{2}{(\omega_s C_1)} = \frac{1}{\pi f C_1} \tag{3.20}$$

For f expressed in MHz and C_1 in pF, this becomes

$$\frac{\Delta X}{\Delta f/f} \approx \frac{10^6}{\pi f C_1}. \tag{3.20a}$$

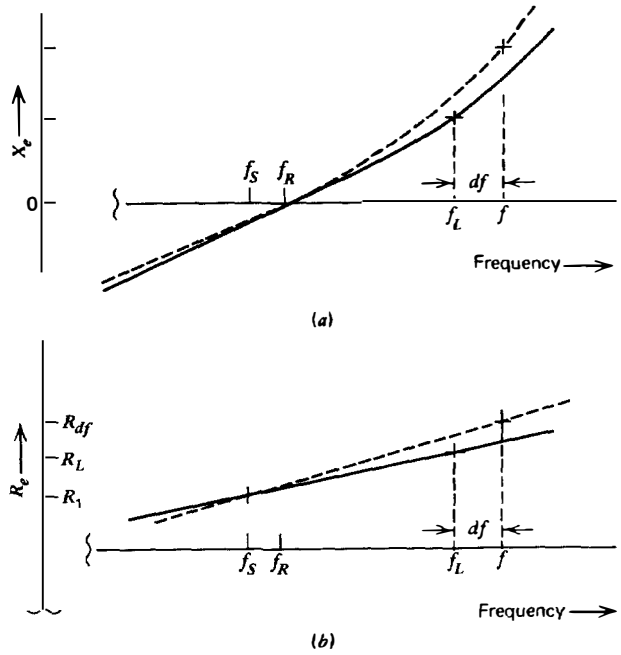

Figure 3.8 Impedance versus frequency. (*a*) X_e in the vicinity of resonance. The solid line is drawn for the case where the static capacitance is C_0; the dashed line represents the case where the static capacitance is increased to C_0'. At the actual operating point the frequency is f, and the value of X_e is X_{df}, corresponding to a static capacitance of C_0'. (*b*) R_e versus frequency in the vicinity of resonance. The solid and dashed lines have the same meaning as in (*a*). At the actual operating frequency (f), the value of R_e is R_{df}.

This expression is, strictly speaking, only accurate in the region close to f_s; we use it as a measure of the slope of the curve at the operating frequency f, although we recognize that it may underestimate the slope by a factor of 2 or 3. The slope of X_e versus frequency is a measure of crystal resonator *stiffness*. Operation of the resonator with C_L is chosen because the slope is increased, and changes in the llator do not affect f as much near f_L as near f_s.

If the crystal resonator, represented by the circuit of Fig. 3.5, is operated with series C_L, then the frequency will be f_L. Unfortunately, there is always additional stray capacitance shunting the crystal enclosure, for example, wiring capacitance. These strays are external to the enclosure and increase the value of C_0 in Fig. 3.5 to a larger value C_0'. Just as C_0 is a specification value, so too is C_0' a specification, but it depends upon the llator as well as C_0. The effects upon X_e and R_e of the change from C_0 to C_0' may be seen in Fig. 3.8, where the dashed lines represent the C_0' influence.

In order to produce the frequency f at which it is desired to operate, given that f may differ by a small amount df from f_L, as shown in Fig. 3.8, it is

necessary to alter the value of the load capacitor from the rated C_L value. This is done with a trimmer capacitor. If, in addition to the shift in frequency by df, the fact that C_0' and not C_0 is the true effective value of static capacitance to be taken into account, then the trimmer will have to accomplish both adjustments. The value of load capacitance required will be denoted $C_{L_{df}}$ and is determined by using Eq. (3.10) to compute the motional arm reactance $X_{1_{df}}$ ($= X_1$ at Δf taken to be $(f_L - f_s) + df$) and then using Eq. (3.16) to substitute for $(f_L - f_s)/f$.

$$X_{1_{df}} \approx \left(\frac{2}{\omega C_1}\right) \cdot \left(\frac{(f_L - f_s)}{f} + \frac{df}{f}\right) \tag{3.21}$$

$$X_{1_{df}} \approx \left(\frac{2}{\omega C_1}\right) \cdot \left(\frac{C_1}{2(C_0 + C_L)} + \frac{df}{f}\right) \tag{3.22}$$

The negative capacitance equivalent to $X_{1_{df}}$ is $(\omega X_{1_{df}})^{-1}$, or

$$\left(\frac{1}{C_0 + C_L} + \frac{2df}{C_1 f}\right)^{-1}, \tag{3.23}$$

and $C_{L_{df}}$ is just this value minus C_0':

$$C_{L_{df}} = \left[(C_0 + C_L)^{-1} + \frac{2df}{C_1 f}\right]^{-1} - C_0' \tag{3.24}$$

With f in MHz, and df in Hz, this is

$$C_{L_{df}} = \left[(C_0 + C_L)^{-1} + 2(10^{-6})\frac{df}{C_1 f}\right]^{-1} - C_0' \tag{3.24a}$$

The value of R_L is given as a specification. From it, the value of R_1 is found from Eq. (3.19). The actual resistance presented by the resonator at the frequency $f_L + df$, taking into account C_0', will be denoted R_{df}. It is determined by using Eq. (3.12) with C_0 replaced by C_0', and with Δf equal to $(f_L - f_s) + df$:

$$R_{df} = R_1\left(1 - \frac{2C_0'[(f_L - f_s) + df]}{C_1 f}\right)^{-2} \tag{3.25}$$

Equation (3.16) is used to eliminate $(f_L - f_s)/f$; after simplification one obtains:

$$R_{df} = R_1\left(1 - \frac{C_0'}{C_0 + C_L} - \frac{2C_0' df}{C_1 f}\right)^{-2} \tag{3.26}$$

With f expressed in MHz and df in Hz, Eq. (3.26) becomes

$$R_{df} = R_1\left(1 - \frac{C_0'}{C_0 + C_L} - \frac{2C_0'\,df}{C_1 f \times 10^6}\right)^{-2} \tag{3.26a}$$

Power dissipation in the crystal is a specified quantity P_x. From P_x and the operating resistance R_{df}, the crystal current I_x follows:

$$I_x = \left(\frac{P_x}{R_{df}}\right)^{1/2} \tag{3.27}$$

When P_x is given in mW and I_x in mA, the relation is

$$I_x = \left(\frac{1000P_x}{R_{df}}\right)^{1/2} \tag{3.27a}$$

A useful general expression, independent of the value of C_0', for the change in reactance with frequency is obtained from differentiating Eq. (3.22) and making use of Eq. (3.24) in the result to obtain[3.12]

$$\frac{\partial X_{df}}{\partial f} = \frac{2Q_x R_{df}}{f} \tag{3.28}$$

The quality factor Q_x is defined in Eq. (3.29); it is a constant for a given unit (see Section 3.2.3.1). R_{df} is the equivalent resistance of the osci at the frequency of measurement, at any value of C_0', and varies from approximately R_1 at f_R up to what is normally many times R_1 at f_A [see Eq. (3.39)]. With the measurement of R_{df} at the operating frequency, the reactance slope is simply and accurately determined by Eq. (3.28); it applies at any frequency in the resonance range.

3.2.3 Figures of Merit[3.11]

This subsection considers a number of figures of merit derived from the equivalent circuit parameters of Fig. 3.5, their importance, and application.

3.2.3.1 The Q Concept

The resonator *quality factor* Q_x is defined by the relation

$$Q_x = \frac{1}{\omega C_1 R_1} = \frac{1}{2\pi f C_1 R_1} \tag{3.29}$$

where $\omega = \omega_s$, or, with f expressed in MHz and C_1 in pF,

$$Q_x = \frac{10^6}{2\pi f C_1 R_1} \tag{3.29a}$$

Using Eq. (3.6), Q_x may be expressed in other equivalent forms, but involves only the parameters of the motional arm; it is the ratio of motional capacitive reactance to resistance at f_s. There is some confusion regarding the meaning and use of Q_x, and this can lead to costly overspecification. The Q concept for resonators has been carried over from its traditional use in connection with resonance in RLC circuits. In this latter case it is shown that the width of the resonance curve is inversely proportional to Q, so that the quality factor measures the *sharpness* of the resonance. With regard to the crystal resonator, the situation is complicated by the presence of C_0 (or C_0'). The frequency interval between resonance and antiresonance is the usual measure of *sharpness* in resonators. This is the region in Fig. 3.7 where X_e is positive. It depends upon the ratio of C_0 to C_1 almost exclusively; this is discussed in Section 3.2.3.3. The presence of loss ($Q_x^{-1} \neq 0$) blunts the extremes of X_e and causes X_e to be zero at the antiresonance point, but these regions are excluded from use in this book.

For filter applications the resonator Q shows up directly in the passband insertion loss. For oscillator applications, which are our concern here, it would appear from what has been said above that Q_x is not involved directly in determining the *sharpness* of the resonance, and hence the oscillator stability. This seems to be at variance with the usual statements regarding the importance of the high Q of quartz vibrators for frequency control. The confusion arises from two sources. First, it is certainly true that if a resonator is going to be operated in its inductive region, as is usually the case, then its frequency must lie within the limits given by the *sharpness* of the X_e curve. However, as seen in Fig. 3.8*a*, if the actual operating frequency is f and the resonator reactance is X_{df}, then any changes in X_e about the X_{df} point brought about by llator changes will produce frequency departures from f by amounts that depend not upon the resonance–antiresonance distance, but upon the slope of X_e at the operating point. Thus the stability is measured in part by Eq. (3.20), and this does not depend upon Q_x, but is rather inversely proportional to C_1.

The second source of confusion regarding Q stems from associating the crystal Q_x with the *operating* Q of the oscillator. The Q_x of the resonator is not the true measure of oscillator stability. The loaded or operating Q determines frequency stability, and this value depends upon both the osci and llator properties. The operating Q is proportional to the reactance slope [see Eq. (3.20)] and hence is determined by C_1; it is always less than Q_x. Because it is sometimes considerably less than Q_x, it will not pay in such cases to put a premium on the resonator Q_x. To do so will mean paying for an attribute that cannot be utilized. Considered from another viewpoint, the llator should be

designed in such a manner that the loaded Q is as high as possible for greatest stability and most efficient use of the resonator Q_x.

The inverse of Q_x is a measure of loss in the vibrator. The loss is generally a combination of three contributions: (1) the internal friction of the crystal, (2) loss of vibratory energy to the mounting supports, and (3) energy loss to the gas within the enclosure. Most modern units are sufficiently evacuated that (3) plays no role. For quartz crystals, Q_x ranges from 10^4 to 10^7, with the lower values obtained at the lower frequencies, below about 1 MHz, because of mounting losses, and also at very high frequencies, above 200 MHz, because of internal friction. Realizable Q_x values are a maximum in the range 2.5 to 5 MHz as a tradeoff between external (mounting support) loss and internal (frictional) loss.

Above about 10 MHz the internal friction losses begin to dominate the Q_x for quartz. For AT-cut overtone units, Q_x is due almost exclusively to internal losses. A considerable portion of these losses arises from defects and impurities in the crystal lattice; these in turn are functions of the growth process and for cultured quartz can vary considerably in manufacture. The internal friction has been found to be correlated with infrared absorption, so a simple IR test during selection of material is used for quality control of Q_x. The Q_x figures are also found to be quite temperature sensitive and can lead to R_1 and R_L changes over operating temperature ranges. The R_L value specified should be the maximum permissible over the desired temperature range.

For AT-cut quartz at room temperature, the maximum intrinsic values of Q_x are found to follow the relation[3.13]

$$Q_x \cdot f \approx 16 \times 10^6 \tag{3.30}$$

where f is in MHz. This relation is independent of overtone. It is given a simple explanation in the next section.

3.2.3.2 *Motional Time Constant τ_1*

Equation (3.29) is of the same form as Eq. (3.30) if the R_1C_1 product is a constant. This is defined as the motional time constant τ_1 with a value corresponding to Eq. (3.30) of

$$\tau_1 = R_1C_1 \approx 10^{-14}\ \text{s} \tag{3.31}$$

This quantity is simply related to the attenuation of an acoustic wave as it travels within the crystal to cause the vibration. It is a function of crystal cut, type, and mode of vibration, but does not vary by more than a factor of 2 or so. It is a function of temperature, but is independent of frequency and overtone as long as the losses arise only from the internal friction. As was stated earlier, this is usually only the case for quartz above 10 MHz where flat plates vibrating in thickness shear are used. These plates are mounted at the

Table 3.1 Frequency and Motional Time Constant, and Piezoelectric Coupling Factor of Popular High-Frequency Quartz Cuts

Cut	Frequency Constant, N_0 (MHz-mm)	Motional Time Constant, τ_1 (10^{-15} s)	Piezoelectric Coupling Factor, k (percent)
AT	1.661	11.8	8.80
SC	1.797	11.7	4.99
BT	2.536	4.9	5.62

edges where the vibratory motion is nearly zero provided the plate diameter-to-thickness ratio is greater than about 50 to 80. For such plates the fundamental frequency is given by

$$f = \frac{N_0}{t} \tag{3.32}$$

N_0, the frequency constant, is given for a number of popular cuts in Table 3.1; t is the plate thickness in mm and f is the nominal frequency in MHz. Values of τ_1 are also given in Table 3.1.[3.7]

As an exercise we will compute the lowest frequency AT-cut that will fit in an HC-6/U holder (Fig. 3.1) such that its Q_x will not be severely degraded by the mounting supports. From Fig. 3.1 we choose a plate diameter of 14 mm to permit room for the mounting posts. Taking $\frac{1}{60}$ of this for the thickness t of the plate, and using Eq. (3.32) and Table 3.1, we get approximately 7 MHz.

For diameter (or width)-to-thickness ratios less than about 60 normally, the mounting supports increase the loss and lead to an effective time constant τ that is described on the average by the relation

$$\tau = \tau_1\left[1 + \left(\frac{60}{d}\right)^2\right] \tag{3.33}$$

In Eq. (3.33), d is the diameter-to-thickness ratio. Continuing our example, if a 7-MHz AT-plate was contained in an HC-18/U holder, then from Fig. 3.2, a value of 7 mm for the diameter would be reasonable. This would give a value for d of nearly 30, and τ would be increased by a factor of 5; Q_x would be 20% of its maximum value at this frequency. Often Eq. (3.33) represents a lower bound of what is achieved in practice by contouring the plate to reduce edge motion (see Section 3.6).

From simple considerations of frequency and dimensions, reasonable estimates of Q_x may thus be found by the use of the motional time constant.

3.2.3.3 *Capacitance Ratio r*

The quantity r is defined as the ratio of the static to motional capacitances

$$r = \frac{C_0}{C_1} \tag{3.34}$$

It is a measure of the antiresonance–resonance (pole-zero) frequency separation that is important in filter applications

$$f_A - f_R \approx \frac{f_R}{2r} \tag{3.35}$$

and is related to a material constant called the piezoelectric coupling factor k which depends upon crystal cut, type, and mode of vibration. For the very popular thickness modes of plates,

$$2r = \left(\frac{\pi N}{2k}\right)^2 \tag{3.36}$$

where $N = 1, 3, 5, \ldots$, is the overtone number (see Section 3.2.4.1).

As was discussed in Section 3.2.2, the resonator is operated at a frequency f situated between f_R and f_A. The pole-zero distance, and hence r, is only important for oscillators to the extent that it qualitatively indicates how *stiff* the resonator is, that is, between what limits f may be *pulled* by a trimmer capacitor. Although it is often cited as one of the most important parameters for oscillator application, the really important parameter is C_1, and not r. One should also bear in mind that it is C_0' and not C_0 alone that must be considered in the oscillator design.

Equation (3.36) discloses that r increases with the square of the overtone order. From Eq. (3.35) we see that overtone units are more suitable for high-stability oscillator application; for temperature-compensated crystal oscillators (TCXOs) and variable crystal oscillators (VCOs) fundamental ($N = 1$) operation is preferred (see Section 3.2.5). Typical r values for quartz range from 100 to 20,000.

In applications where a capacitor in series with the crystal unit is varied for purposes of modulation or temperature compensation, the frequency–temperature behavior (see Section 3.7) will change somewhat with operating frequency. This effect is due to the temperature coefficient of k in Eq. (3.36) and must be accounted for in precision applications.

3.2.3.4 *Figure of Merit M*

The figure of merit M is defined as

$$M = \frac{Q_x}{r} \tag{3.37}$$

For quartz vibrators it ranges from less than unity to 10,000. Its chief use is to indicate when a vibrator ceases to possess an inductive region, that is, when f_R and f_A no longer exist as the zeros of X_e. Equation (3.35) is not valid if M becomes too small. In this case a more exact formula must be used that takes into account the blunting of the X_e curve by the finite Q_x around the maximum and minimum of X_e. It happens that when

$$M \leqslant 2 \tag{3.38}$$

the X_e curve no longer becomes positive (inductive), so f_R and f_A fail to be defined, and the analysis of Section 3.2.2 cannot be used. Because Q_x decreases with increasing frequency from Eq. (3.30), and r increases with the square of the harmonic number, from Eq. (3.36), there is a tradeoff to be considered for high-frequency resonators between use of high harmonics for increased stability, and the resulting rapid decrease in M. See Section 3.2.4.1. The maximum value of R_e occurs close to f_A and has the value

$$R_e(\text{maximum}) \approx R_1 M^2 \tag{3.39}$$

3.2.4 Typical Parameter Values

Ranges of parameter values for quartz resonators are given in this subsection. All generally used cuts and types of vibration are considered, including the increasingly important SC-cut, with the exception of SAW devices (see Section 3.4), and miniature resonators (see Section 3.5). Additional information on SC-cuts is given in Section 3.3.

3.2.4.1 Overtones

Most types of vibration may be used on different overtones or harmonics. The most popular by far are the thickness vibrations of plates such as AT- and BT-cuts of quartz, where the thickness determines the fundamental frequency by Eq. (3.32). Odd overtones of this frequency may be excited in resonators as well, and for the overtone family of resonances of a given type the parameters of the equivalent circuit are simply related.

Figure 3.9 is the equivalent circuit of Fig. 3.5 extended to represent the family of overtones associated with the fundamental. C_0, C_1, L_1, and R_1 are unchanged in value from Fig. 3.5, but, as may be inferred from Eq. (3.36),

$$C_N = \frac{C_1}{N^2} \tag{3.40}$$

Since the frequency of the Nth overtone is N times the frequency of the fundamental, it follows from Eq. (3.6) that

$$L_N = L_1 \tag{3.41}$$

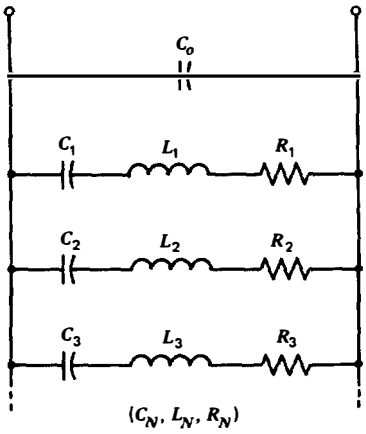

Figure 3.9 Equivalent circuit of Fig. 3.5 extended to represent overtones. Each series arm accounts for one resonance, in the vicinity of which the other arms may be neglected. In the region of the Nth, overtone the circuit is accurately represented by C_0 plus C_N, L_N, and R_N.

Finally, from Eq. (3.31),

$$R_N = R_1 N^2 \tag{3.42}$$

As was mentioned in Section 3.2.3.3, overtones are used because the smaller C_N values lead to greater frequency stability because, by Eq. (3.20), the reactance slope increases with increasing N. The present discussion has considered only overtones belonging to a single family. In practice a number of families of types and modes of vibration are simultaneously present in the spectrum of the resonator, and the spectrum is usually more cluttered with unwanted responses as N increases. Special designs have been worked out to reduce the unwanted responses at a desired overtone. For this reason a crystal is usually designated for operation at a specific N and should be used only at this overtone for best results. This subject will be considered further in Sections 3.3 and 3.6.

3.2.4.2 Circuit Parameter Ranges for Quartz

Typical ranges of frequency and equivalent circuit parameters for traditional cuts of quartz and types of vibration are given in Table 3.2. Additional values for the newer miniature resonators are given in Section 3.5. Table 3.2 data of C_1 and R_1 are shown graphically in Figs. 3.10 and 3.11 as functions of frequency. Boundary lines are only approximate, and for special applications the boundaries may be stretched considerably. For example, recent developments of high-frequency plates have pushed the upper limit for fundamental AT-cut resonators well beyond 200 MHz.

From Figs. 3.10 and 3.11 we find two useful rules of thumb:

$$C_1 = 0.1 \text{ to } 0.001 \text{ pF} \tag{3.43}$$

Table 3.2 Quartz Vibrator Parameter Ranges

Cut	Type of Vibration	Frequency Range (MHz)	Approx. C_0/C_1	Range of C_1 (10^{-3} pF)	Range of R_1 (Ω)	Remarks
XY	Flexure	0.001–0.05	600	1–100	10^3–3×10^5	See Section 3.5 for frequency ranges and typical parameters of miniature resonators
NT	Flexure	0.005–0.14	900	1–30	10^3–3×10^5	
5°X	Extension	0.04–0.20	130	20–800	20–5000	
CT	Face shear	0.15–0.85	350	2–100	30–8000	
DT	Face shear	0.10–0.50	400	3–200	30–8000	
GT	Coupled extension	0.08–0.30	350	10–25	40–300	
SL	Face shear/ flexure	0.35–0.70	400	2–100	30–8000	
BT	Thickness shear	3–30	650	20–200	2–500	Fundamental
AT	Thickness shear	0.50–5	450–300	2–100	5–500	Fundamental
AT	Thickness shear	5–30	180–250	5–200	2–100	Fundamental
AT	Thickness shear	10–75	250×3^2	0.5–20.0	5–200	Third overtone
AT	Thickness shear	50–150	250×5^2	0.3–2.0	5–200	Fifth overtone
AT	Thickness shear	100–200	250×7^2	0.2–1	10–300	Seventh overtone

and

$$f \cdot R_1 = 10 \text{ to } 1000\ \Omega \text{ MHz} \tag{3.44}$$

with f expressed in MHz. These ranges hold from 1 kHz to over 50 MHz. In the absence of any additional information, good practical averages for R_1 and C_1 over these frequencies are

$$C_1 = 0.01 \text{ pF} \tag{3.45}$$

and

$$R_1 = \frac{100}{f} \tag{3.46}$$

One sees that these equations lead to time constant values that exceed the minimum [Eq. (3.31)] by factors of 1000 at 100 kHz, 100 at 1 MHz, and 10 at 10 MHz. Mounting losses are largely responsible for the high τ values; this is particularly true for low frequencies, but even for AT-plates the use of large electrodes to obtain a specified C_1 leads to vibratory motion at the plate edges and energy loss to the mounting supports. The data in Fig. 3.11 are for evacuated enclosures. Unevacuated units at frequencies below 0.5 MHz possess R_1 values that run about a factor of 2 higher than the upper limits in the figure, down to about a factor of 10 times higher than the lower limits in the figure. For example, at 20 kHz, R_1 ranges from about 1000 to 300,000 Ω in evacuated

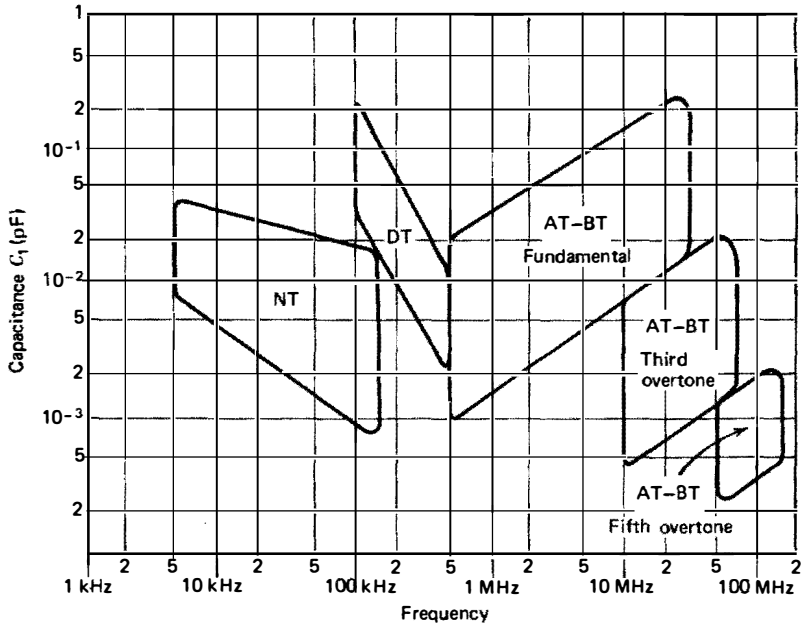

(*a*)

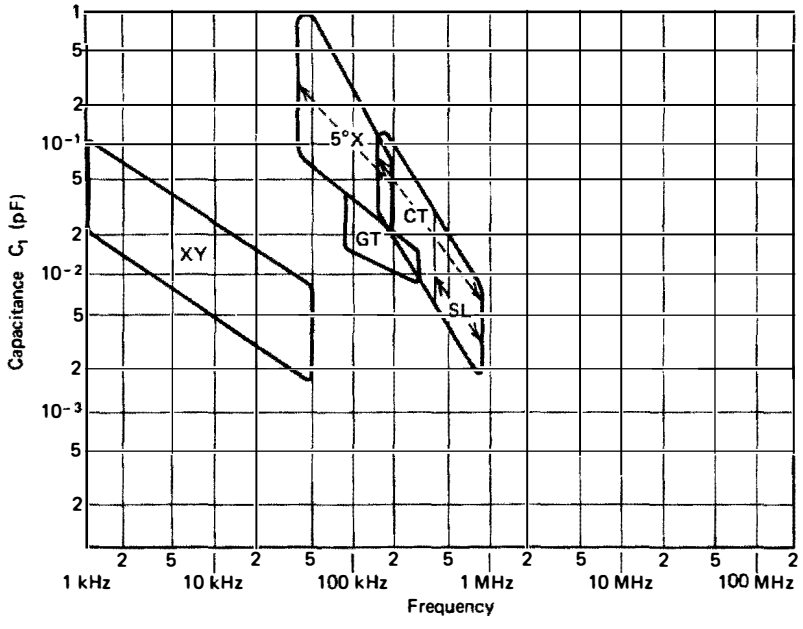

(*b*)

Figure 3.10 Typical ranges of motional capacitance C_1 in picofarads versus frequency. (*a*) For NT, DT, AT, and BT quartz cuts. (*b*) For XY, 5°X, GT, CT, and SL quartz cuts.

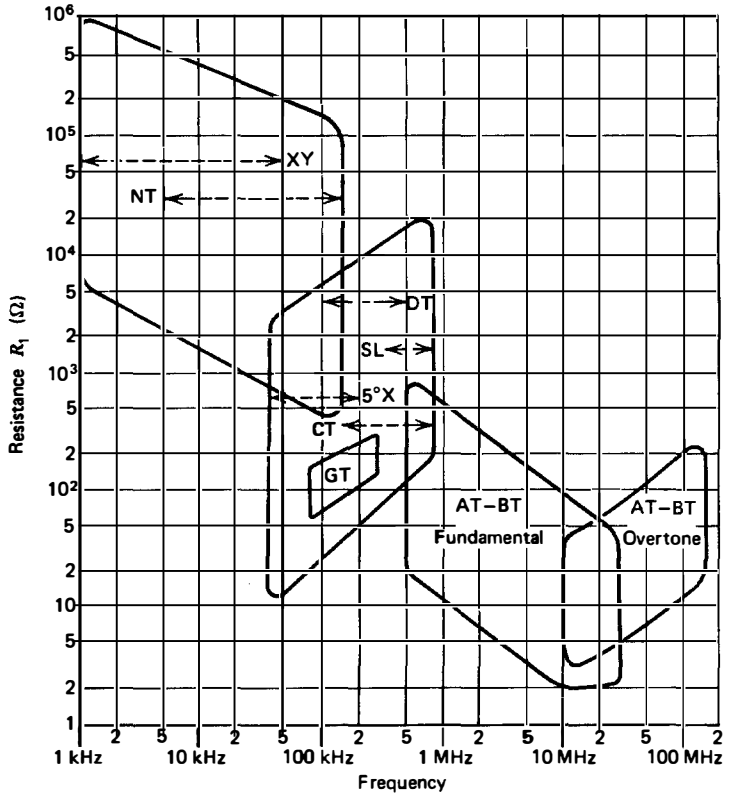

Figure 3.11 Typical motional resistance R_1 versus frequency ranges for NT, XY, 5°X, CT, DT, SL, GT, AT, and BT quartz cuts.

enclosures, and from about 8000 to 600,000 Ω in unevacuated enclosures. At frequencies above 0.5 MHz, the resistance change is about a factor of 2 at both the upper and lower resistance limits.

For the SC-cut one may arrive at parameter ranges using Table 3.2 and Figs. 3.10 and 3.11 for the AT-cut, by dividing the C_1 values by three and taking three times the R_1 values. These estimates follow from Table 3.1 and Eq. (3.36), and the fact that the dielectric constant of quartz determining C_0 is nearly independent of cut. Since the ratio of the squares of the coupling factors is about 3, the ratio of the r values is also; this is then the C_1 ratio since C_0 does not change for comparable resonator design geometry. The time constants are likewise approximately equal, so the resistance ratio follows. The above estimates neglect an 8% difference in plate thickness for similar AT and SC vibrators of the same frequency.

3.2.4.3 Preferred C_1 Values for AT- and SC-Cuts

Achievable motional capacitance values at different frequencies are given in Fig. 3.10 for standard crystal resonators. In different frequency ranges, size

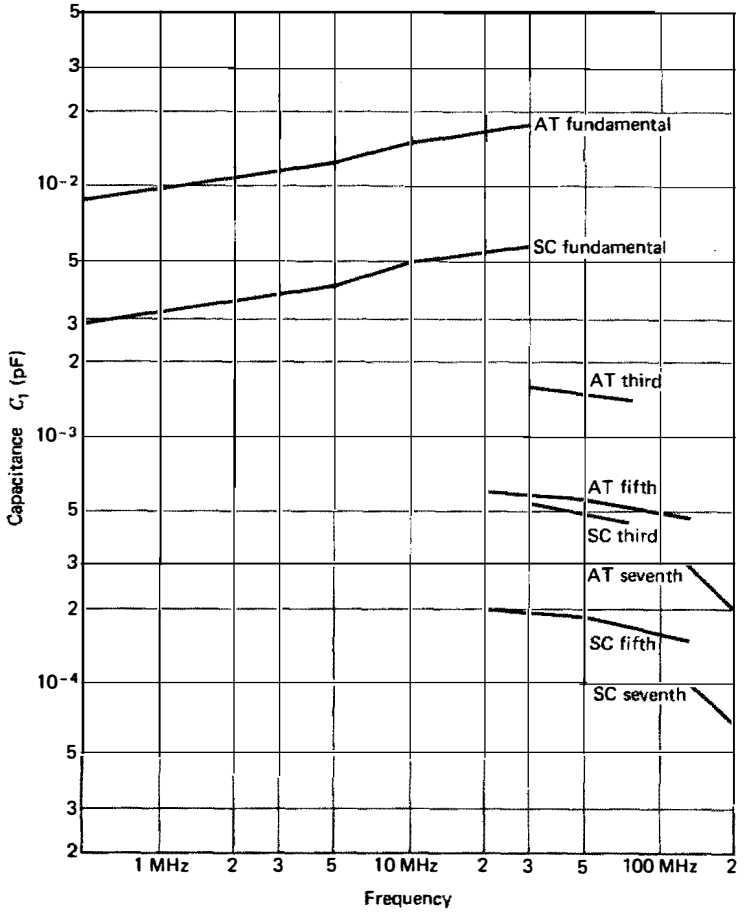

Figure 3.12 Preferred values of motional capacitance C_1, as functions of frequency and overtone, for AT and SC quartz cuts. Designs in a band about these values are most readily and economically produced and lead to the most cost-effective units.

and other considerations lead to the most economical designs if the C_1 values are limited to the preferred numbers indicated in Fig. 3.12. This figure is drawn for the predominantly used AT-cut and the newly introduced SC-cut that is becoming increasingly important for high precision applications. The figure may also be used to approximate the BT-cut by using the AT values; for other cuts and types of vibration, Fig. 3.10 is used to obtain approximate values by taking the range midpoints at each frequency.

Once a design C_1 value has been selected, the corresponding R_1 value can be estimated roughly from Fig. 3.11, or from Eq. (3.33) if the plate geometry is known.

An Illustrative Example

To summarize some of the developments of Sections 3.2.3 and 3.2.4 and to make additional illustrative points of a practical nature, we take as an example an AT-cut resonator with the following measured parameters:

$f = 5$ MHz
$Q_x = 750{,}000$
$R_1 = 4\ \Omega$
$C_0 = 5.04$ pF.

The above equivalent circuit quantities are measured at the crystal enclosure terminals. From Eqs. (3.29) and (3.31) we obtain

$$C_1 = 10.6 \times 10^{-3}\ \text{pF}$$

$$\tau_1 = 42.4 \times 10^{-15}\ \text{s}$$

and Eq. (3.6) gives

$$L_1 = 95.5\ \text{mH}.$$

The C_0 value includes stray capacitance associated with the holder, but does not include strays that may be associated with the using circuitry. The capacitance ratio including resonator strays is

$$r = \frac{C_0}{C_1} = 475$$

This resonator is obviously a fundamental unit because if the k value from Table 3.1 is used in Eq. (3.36), it predicts a ratio, r_0, of 159 for the fundamental, and 1434 for the third overtone. Since 475 is less than the third overtone value, it must be a fundamental. The value of 475 is about three times higher than the theoretical value. This comes about for two reasons. First, presence of stray capacitance makes C_0 larger than the C_{10} that arises from the parallel-plate capacitor structure consisting of the crystal plus electrodes. Second, the value of k in Table 3.1 is a material constant for AT-cut quartz, whereas the k in Eq. (3.36) is an effective value that is reduced by a geometrical factor Ψ (less than 1) to account for the fact that the mechanical vibratory motion of the crystal plate is not of equal amplitude over the entire electrode area where the piezoelectric current is collected. When low r values are desired (see Section 3.2.5) a compromise is often necessary between having a relatively uniform distribution of motion over the electrodes, and having the motion taper off near the electrode edges so that the plate edges will be quiet. Then little energy is lost to the mounting supports, degrading τ_1, and hence R_1.

The rules governing the distribution of motional activity are called *energy trapping* laws and are touched upon in Section 3.6.

The figure of merit and maximum of R_e follow from Eqs. (3.37) and (3.39):

$$M \approx 1579$$

$$R_e(\text{maximum}) \approx 10 \times 10^6\ \Omega$$

Equation (3.35) determines the pole-zero separation as

$$f_A - f_R \approx 5.26\ \text{kHz}$$

If the resonator is operated with load capacitance C_L of 32 pF, the frequency shift from f_R will be, from Eq. (3.16),

$$f_L - f_R \approx 716\ \text{Hz}$$

and the load resistance follows from Eq. (3.19) as

$$R_L \approx 5.3\ \Omega$$

Normally this will be specified and R_1 will be derived. Using Eq. (3.32) the plate thickness is

$$t \approx 0.332\ \text{mm}$$

At this point little further of an electrical nature may be determined without looking within the resonator enclosure. We will assume the following physical attributes:

Enclosure: HC-6/U
Plate diameter: $D = 14$ mm
Electrode diameter: $D_e = 5.6$ mm

With this additional information we are able to determine

$$d = \frac{D}{t} \approx 42.2$$

which, from Eq. (3.33), yields the estimate

$$\tau \approx 35.7 \times 10^{-15}\ \text{s}$$

this compares with 42.4 fs computed from the R_1C_1 product and discloses that with greater attention to mounting the R_1 could be reduced somewhat. Such a specification could result in much greater cost and would be of doubtful utility

since C_1, the more important parameter, is almost unaffected by the mounting loss.

The average dielectric permittivity of quartz is

$$\varepsilon \approx 40 \times 10^{-3} \text{ pF/mm}$$

and the static capacitance C_{10} of the electrodes is therefore

$$C_{10} = \frac{\varepsilon \pi D_e^2}{4t} \approx 3 \text{ pF}$$

The stray capacitance due to the mount and enclosure is approximately

$$C_{\text{stray}} = C_0 - C_{10} \approx 2 \text{ pF}$$

and the true capacitance ratio, excluding the strays, is

$$r = \frac{C_{10}}{C_1} \approx 280$$

With the effect of strays excluded, we may estimate the geometrical factor Ψ that measures the distribution of motion under the electrodes compared to the ideal case of uniform amplitude where Ψ is unity:

$$\Psi = \frac{r_0}{r} = \frac{159}{280} \approx 57\%$$

The Ψ value varies with D/t and D/D_e ratios, as well as electrode thickness and plate contour (see Section 3.6). In theoretical calculations of resonator equivalent circuit parameters, ideal values for $\Psi = 1$ are obtained. Then a realistic value of Ψ is obtained from the particular design at hand. This leads to effective values by multiplying the theoretical C_1 values by Ψ and dividing both L_1 and R_1 quantities by this factor. C_0 is unaffected by the motional distribution.

3.2.4.4 Some Standard Units Designed for Operation with Load Capacitor C_L

Table 3.3 lists typical values associated with standard crystal units designed to operate with load capacitance C_L as tabulated. These are described by CR number (see Ref. 3.62) and are referred to in the popular literature as *antiresonant* units. From the discussion in prior sections we see that this designation is not correct; the units operate near f_L and not f_A and should more properly be called *load-resonant* units. In Table 3.3 the units selected are all fundamentals, with the exception of the third overtone CR-33/U entries, and the fifth overtone CR-71/U unit. Standard crystal units have not yet been

Table 3.3 Typical Values of Standard Units Designed to Operate with Load Capacitor C_L

CR Number	Cut	f (MHz)	C_0 (pF)	C_L (pF)	R_L (ohms)	R_1 (ohms)	r	C_1 (10^{-3} pF)	Q (10^3)	M
18	AT	1	7	32	575	388	250	28	14.7	59
27	AT	5	7	32	60	40	250	28	28.4	114
36	AT	10	7	32	24	16	250	28	35.5	142
62	AT	20	7	32	20	13	250	28	21.9	88
29	DT	0.200	11	32	6000	3,324	400	27.5	8.7	22
33	AT	10	12	32	65	34	2,500	4.8	97.5	39
33	AT	25	12	32	17	9	2,500	4.8	147.	59
36	AT	0.800	7	32	625	421	250	28	16.9	68
37	5°X	0.090	6.2	20	5000	2,910	120	51.7	11.8	98
37	5°X	0.250	2.5	20	5500	4,345	120	20.8	7.0	59
38	NT	0.016	7.6	20	110,000	57,860	900	8.4	20.4	23
38	NT	0.100	4	20	90,000	62,460	900	4.4	5.7	6
42	5°X	0.090	6.2	32	4500	3,159	120	51.7	10.8	90
42	5°X	0.250	2.5	32	5000	4,305	120	20.8	7.1	59
57	CT	0.500	7	32	3000	2,022	350	20	7.9	23
68	AT	3	7	32	40	27	250	28	70	281
71	AT	5	4	32	150	119	35,000	0.11	2341	67

established incorporating SC-cuts (see Section 3.3), SAW resonators (see Section 3.4), or miniature resonators (see Section 3.5), but will in the future.

3.2.4.5 Some Standard Units Designed for Operation near f_R

Table 3.4 lists typical values associated with standard crystal units designed to operate near f_R. These are referred to in the popular literature as *series resonant* cuts, indicating that the llator series capacitance is very large ($C_L^{-1} \to 0$). In addition to the circuit values, the operating temperature range is given; the resistance figure is a maximum value over the temperature range. Where a single temperature is listed, the unit is designed to be operated in an oven at that temperature. The frequency deviation column ($\Delta f/f$) lists the rated frequency tolerance, in parts per million, for the unit due to the sum of all environmental disturbances, for example, temperature, vibration, and so on.

In both Tables 3.3 and 3.4, a C_0 value of 7 pF is often given for AT-cut units. This value occurs as a maximum limit of C_0 for most standard AT units and was established at one time along with minimum R_1 values in order to guarantee sufficient Q_x and reactance slope.

3.2.5 Circuit Modifications

This subsection deals with frequently used resonator circuit alterations. The changes are made to the circuit of Fig. 3.5 either by the deliberate addition of

Table 3.4 Typical Values of Standard Units Designed to Operate near f_R

CR Number	Cut	f (MHz)	C_0 (pF)	R_1 (Ω)	r	C_1 (10^{-3} pF)	Q (10^3)	M	T^a (°C)	$\Delta f/f^b$ (10^{-6})
50	NT	0.100	4	60,000	900	4.4	6.0	7	−40 to +70	±20
26	DT	0.300	9	4,000	400	22.5	5.9	15	+75	±20
45	DT	0.455	5	3,300	385	13	8.2	21	−40 to +70	±200
19	AT	0.800	7	520	300	23.3	16.4	55	−55 to +105	±50
157	AT	5	7	37	180	38.9	22.1	123	−55 to +105	±50
79	AT	10	7	30	200	35	15.2	76	−55 to +105	±50
79	AT	20	7	20	250	28	14.2	57	−55 to +105	±50
65	AT	20	7	40	2150	3.3	60.3	28	+75	±10
84	AT	60	7	40	2300	3.0	22.1	10	+85	±20
67	AT	30	7	40	2200	3.2	41.4	19	−55 to +105	±25
81	AT	65	7	40	2100	3.3	18.5	9	−55 to +105	±50
74	AT	125	4.5	25	5800	0.78	65.3	11	+80 to +90	±10
80	AT	50	7	50	6250	1.1	57.9	9	−40 to +90	±20
80	AT	95	7	60	5700	1.2	23.3	4	−40 to +90	±20
82	AT	80	7	50	6000	1.2	33.2	6	−55 to +105	±50

[a]Operating temperature range.
[b]Frequency tolerance over temperature range.

other circuit elements, or because of the intrinsic properties of the crystal unit under consideration.

3.2.5.1 Addition of a Series Element and/or a Parallel Element

Figure 3.7 shows the crystal series reactance plotted over a wide frequency range. The reactance slope is relatively small and constant from somewhat below to the immediate vicinity of f_R, and increases steadily in the inductive region above f_R. As discussed earlier, operation at f_L in the inductive region leads to greater frequency stability because of the higher reactance slope; incidental changes in llator reactance produce smaller frequency changes about f_L than about f_R.

Variable crystal oscillators (VCOs) are an example where operation is desirable in the region of lower reactance slope, that is, at, or somewhat below, f_R. Changes in the osci total series reactance in this region will produce the largest frequency shifts for a given reactance change (greatest "pullability"). Figure 3.13*a* shows schematically the crystal unit alone, and Fig. 3.13*b* shows the resonator with series inductor. Looking at the total series reactance of inductor plus crystal as a function of frequency in a narrower range centered about f_R gives the result sketched in Fig. 3.14 for "series inductor." It is the solid "crystal alone" curve translated upward by the inductor reactance, which may be considered constant over this narrow frequency range. If, instead, a

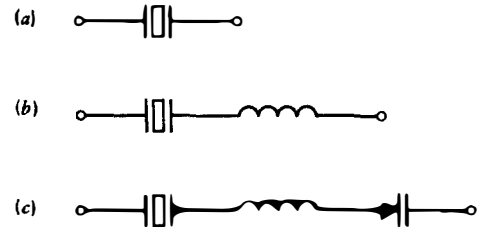

Figure 3.13 (*a*) Crystal resonator. (*b*) Resonator with series inductor. (*c*) Resonator with inductor and varactor in series to adjust the frequency of operation for modulation and compensation applications.

series capacitor is used, the osci total reactance will be reduced at each frequency. This is shown in Fig. 3.14 by the "series capacitor" curve, drawn here for the case of capacitor reactance magnitude equal to that of the inductor. When both inductor and capacitor are placed in series with the resonator, the resulting reactance curve is determined by the sum of the reactances; in particular, if the capacitor is a variable reactance (varactor), as in Fig. 3.13*c*, operation may be made to take place in the region near f_R where the relatively small reactance slope produces large frequency shifts for given varactor changes made for purposes of frequency modulation, temperature compensation, and so on.

By definition, the osci consists in this case of the crystal network—the resonator plus inductor plus varactor, although for practical measurement purposes it might be advisable to include the varactor with the llator.

Inclusion of an inductor in series with the resonator has, in general, two broad functions. The first, discussed above, is to permit the crystal to operate

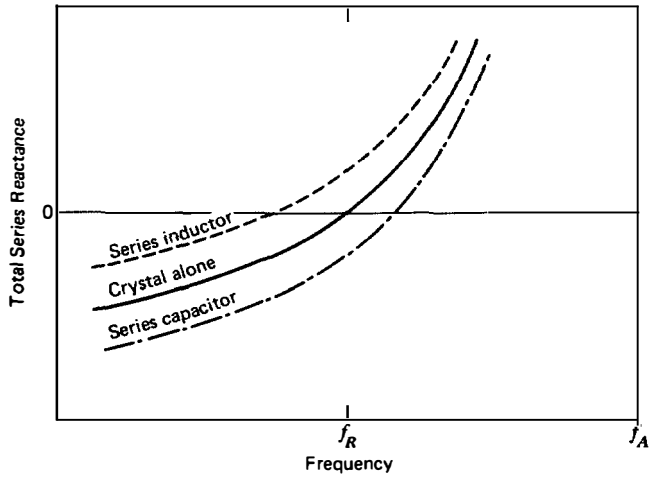

Figure 3.14 Reactance versus frequency for oscis consisting of crystal plus series inductor (short-dashed curve) and crystal plus series capacitor (long-dashed curve).

in the region around f_R where the reactance slope is small, so that large "pullability" is achieved. The second function served by a series inductor is to force the crystal network to look inductive in those applications where it must look inductive, for example, in the Pierce family of oscillators. The resonator may not become inductive at high overtones (see Sections 3.2.3.4 and 5.3.5, item 2).

The heart of the oscillator is the crystal; it should be operated in the frequency region at, or near, f_L. Deficiencies in crystal manufacture, such as poor lapping and plating tolerances resulting in f_L values that deviate from specifications, can be corrected only to a very limited extent by circuit changes, and only at the expense of performance, such as decreased pullability. This situation becomes more critical for units with high r values, especially overtone units. Crystal resonator manufacturing tolerances exert a pervasive influence on the performance of the using oscillator.[3.69]

An inductance is sometimes placed in parallel with the crystal to *antiresonate* C_0. When this is done f_R is unchanged, but the pole is moved upward in frequency, increasing the separation and reducing the apparent capacitance ratio.

3.2.5.2 High-Loss Quartz and Ceramic Resonators

In lower-frequency applications where moderate stability can be used and where cost is an overriding consideration, ceramic resonators are often the choice. They are made of polycrystalline ferroelectric materials in the barium titanate and zirconate families. The ceramic mixture is formed to its desired shape and converted to an artificial piezoelectric by slow cooling from a temperature above the ferroelectric transition point in the presence of a strong electric field. In a manner analogous to the formation of a magnet by aligning molecular dipoles in a strong field, the molecular electric dipoles are oriented. When the high voltage is disconnected from the cooled sample, the preferential orientations of the electric dipoles of the polycrystalline aggregate yield a permanent electric moment which is equivalent to the presence of piezoelectricity.

The equivalent electrical circuit of a ceramic resonator is shown in Fig. 3.15. It is the same as that in Fig. 3.5 except for the addition of the shunt resistance R_0. It comes about from the presence of dc conduction paths around the polycrystalline domains and is intrinsic to the material. The circuit of Fig. 3.15 is sometimes encountered with quartz resonators when there is a leakage path between terminals resulting from faulty construction or damage to the enclosure.

Table 3.5 lists a set of typical ceramic resonator parameters.[3.8] For ordinary applications the frequency range of ceramics ranges from tens of kHz to about 10 MHz. Q_x values vary between 80 and 1000, while r values between 1 and 80 may be achieved. Figure of merit values range from 1 to 12. Because of the high coupling values that may be obtained (low r values), ceramics are suitable

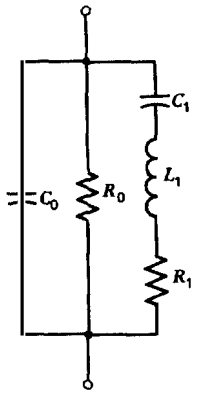

Figure 3.15 Equivalent circuit of a ceramic resonator. In the limit of high dc resistance it becomes Fig. 3.5 for highly insulating dielectric crystals such as quartz.

for medium and wideband low-loss filters. One drawback of these elements is their temperature coefficient of frequency, which is large, being in the range -40 to -80 parts per million per °C. For wideband applications this is not a severe limitation, but for narrowband oscillator application temperature regulation or compensation would more than cancel any cost savings of the element over a corresponding quartz unit.

3.2.5.3 Multimode Resonators

The resonator circuit of Fig. 3.5 is modified by the intrinsic presence of additional modes of motion. These will be treated in Sections 3.3 and 3.6.

3.3 DOUBLY ROTATED CUTS

In the range 0.5 to 200 MHz the resonator of choice is the thickness shear plate. At present the AT-cut accounts for more than 90% of the usage, but for

Table 3.5 Typical Ceramic Resonator Parameters

Quantity	Value	Unit and Remarks
f	452	kHz
C_1	15	pF
r	12.3	C_0/C_1 (often 2 to 30)
R_1	25	Ω
R_0	190	kΩ
Q_x	940	Generally 80 to 1000
$\Delta f/f$	0.003	Temperature stability (20–60°C)
$\Delta f/f$	0.0013	Time stability
$\Delta k/k$	−0.016	per
$\Delta Q_x/Q_x$	0.015	decade
ac depoling	> 1	kV/mm

high- and moderate-precision applications the SC-cut promises to become increasingly popular. The AT-cut is a member of the family of singly rotated cuts; it is formed by aligning the plane of the saw blade with the X-Z crystal axes, and then rotating the blade about the X axis until the angle is reached where the resulting quartz slice has good frequency–temperature properties. Two such cuts exist, the AT-cut with angle $\theta \approx +35°$ and the BT-cut with angle $\theta \approx -49°$. These single rotations are the same as the carpenter's *miter cuts*. The more general case of doubly rotated cuts is obtained by starting, as before, with the blade of the saw aligned with the X-Z crystal axes; the blade is then rotated about its Z axis by an angle ϕ. This first rotation leaves the blade in the X'-Z plane. The second rotation, by angle θ, takes place about the new X' axis. Doubly rotated cuts correspond to the carpenter's *compound cuts*.

Singly rotated quartz cuts with electrodes on the major faces vibrate in thickness shear, with motion along the X axis and acoustic waves travelling in the thickness direction at resonance. In doubly rotated plates three families of motions are in general produced piezoelectrically. These are called the a, b, and c modes, and correspond respectively, to thickness extension, fast thickness shear, and slow thickness shear waves. When $\phi = 0°$ (the singly rotated cuts), the piezoelectric coupling coefficients driving the a and b modes are zero; only the c (slow shear) mode is driven. This mode, with its overtones, was shown earlier to be represented by the circuit of Fig. 3.9. Apart from the static C_0, any mode may be represented by the network of Fig. 3.16*a*. When three mode families are piezoelectrically excited, the complete circuit is that given in Fig. 3.16*b*.

In Fig. 3.16*b*, each mode has the parallel string of series arms as seen in Fig. 3.16*a*. The three families are distinguished in resonance frequencies, mode strengths, and pole-zero distances as described below.

Consider the fundamental of each mode first. Corresponding to each mode will be a separate piezoelectric coupling factor. By Eqs. (3.34) and (3.36) each mode will have its own particular value of motional capacitance. Because the waves travel at different speeds, each mode will have a different frequency constant (the frequency constant is equal to one-half the wave velocity). From Eq. (3.32), the modal frequencies will differ, and, by Eq. (3.6), the inductances will also be different. The loss is usually unequal for each mode as well; this is reflected in three unequal time constants, which, by Eq. (3.31), leads to three differing resistance values.

When the overtones of each mode are considered, Eqs. (3.40), (3.41), and (3.42) determine the remaining circuit elements in Fig. 3.16.

The SC-Cut

As the angle ϕ is increased from zero (AT-cut), if θ is kept approximately constant, it is found that the resulting cuts have relatively good frequency–temperature behavior, but several other things also take place. First of all, the strengths of the a and b modes increase from zero, while the strength of the c mode decreases. The separation of the three modes change, as well as

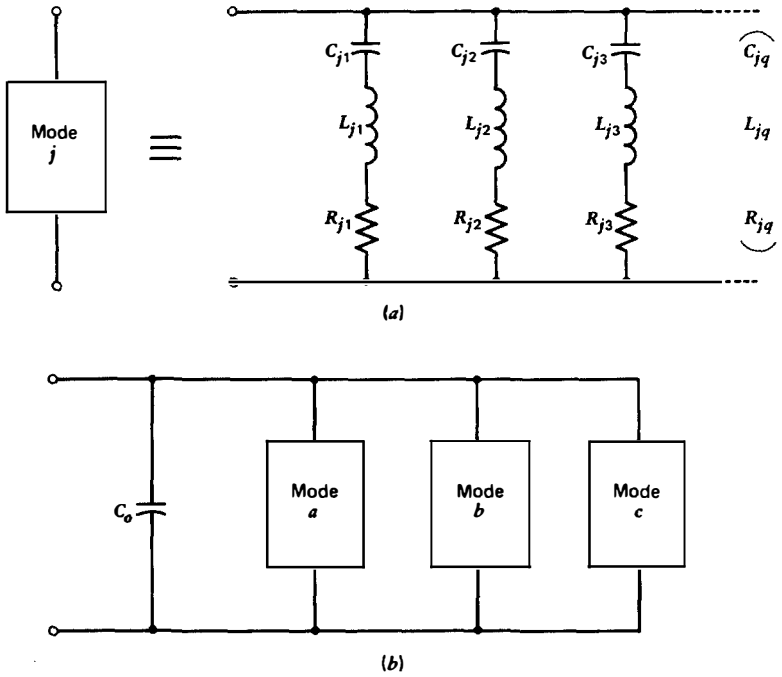

Figure 3.16 (*a*) Motional arms representing the fundamental and overtones of one mode. The overtone elements are related to those of the fundamental by Eqs. (3.40), (3.41), and (3.42). (*b*) Complete equivalent circuit for the thickness modes of a doubly rotated plate such as the SC-cut. Each mode has the circuit representation of the (*a*) part of the figure. The fundamental motional arms differ for each mode; the overtone relations given in (*a*) hold for each mode separately.

the absolute frequencies. The most important changes that take place, from the standpoint of precision resonators, as ϕ is varied, are the changes in sensitivity to electrode stresses and to thermal transients (see Section 3.9). At $\phi \approx 21.9°$ the *c*-mode stress sensitivity becomes zero, and this is the orientation of the SC (stress compensated) cut.[3.15]

Figure 3.17 is a theoretically calculated mode spectrograph of an SC-cut.[3.7] For various practical purposes, such as controlling the temperature coefficient, the ϕ and θ angles vary somewhat in design, so the figure is to be regarded as somewhat variable in mode separations. The frequency of each resonance is indicated above the peak, normalized to the fundamental of the *c* mode. The modal attenuations are much more variable than the frequencies; these can be modified in manufacture, for example, by bevelling or contouring, whereas the calculations are for a flat plate with uniform motion ($\Psi = 1$); these are indicated adjacent to each resonance and are in dB.

The separation between the *b*- and *c*-mode fundamental resonances normally ranges from 8.5 to 10%; the mode strengths will likewise vary by ± 5 dB

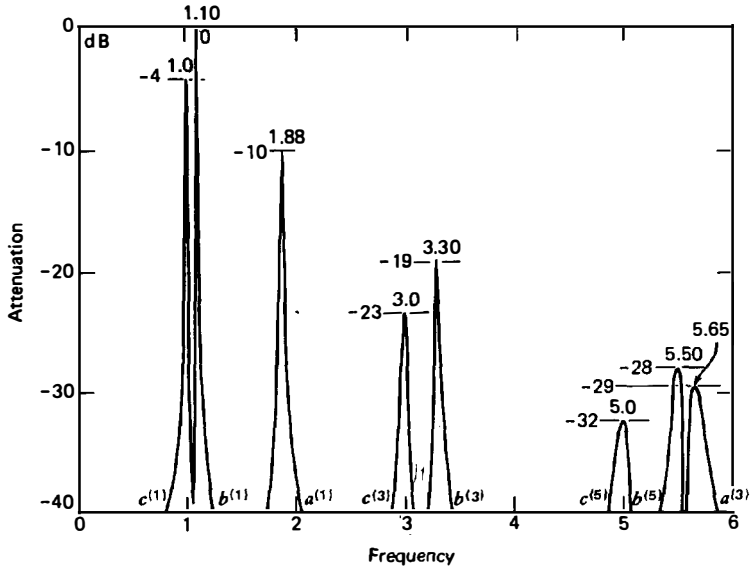

Figure 3.17 Mode spectrograph of an SC-cut showing the complications that arise from the multimode situation. The Nth overtone of mode m is labeled $m^{(N)}$. At the top of each resonance peak is the frequency of the mode, with $c^{(1)}$ taken as unity. The theoretically calculated attenuations are noted at the sides of the peaks; these are in dB. In practice the amplitudes will vary with design, sometimes considerably. The frequency separations will also vary with change in angle ϕ.

with respect to each other. The c-mode SC is about 10 dB weaker than the AT-cut having the same frequency and electrode area.

When designing with SC-cuts, it is of great practical importance to realize that a unit designed for one overtone is not necessarily useful for another overtone. The mode spectrum of resonances and their strengths have to be considered carefully. It may be that a simple mode selection circuit in the llator will suffice for operation on overtones of the stress-compensated c mode. This will be considered further in the circuitry sections.

At present the SC-cut has not been subjected to standardization, but a number of designs at standard frequencies are commercially available. Table 3.6 compares precision AT and SC units.[3.14] Both types are operated in an oven, the AT at its higher-temperature zero temperature coefficient point and the SC at its lower point (see Section 3.7). These units begin to approach the limiting τ_1 values and show attention to this aspect of design; all units are in holders of the HC-6/U size.

SC cuts are more difficult to x-ray than ATs, but this cost factor will diminish considerably with the advent of microprocessor-controlled *smart* x-ray machines currently being developed. From a material point of view, the piezocoupling produces resonances in the SC c mode that have about one-third

Table 3.6 Parameter Values for Precision AT and SC Units

f (MHz)	Cut/ N	C_0 (pF)	R_1 (ohms)	r	C_1 (10^{-3} pF)	Q (10^3)	M	T^a (°C)	$\Delta f/f^b$ (10^{-6})	T_i^c (°C)
5	SC/1	6.8	7	1545	4.4	1033	669	+30 to +75	±10	+100
5	AT/3	3.1	30	5167	0.60	1768	342	+60 to +90	±2	+26
5	SC/3	3.6	85	20,000	0.18	2080	104	+30 to +75	±1.5	+98
10	AT/3	5.0	15	4167	1.2	884	212	+60 to +90	±4	+26
10	SC/3	5.2	55	14,857	0.35	827	55.7	+30 to +75	±1.5	+95
10	AT/3	5.0	12	2273	2.2	603	265	+60 to +90	±4	+26
10	SC/3	5.2	35	6933	0.75	606	87.4	+30 to +75	±3	+95
10	AT/5	3.7	75	18,500	0.20	1061	57.4	+60 to +90	±1.5	+26

[a] Lower turning point range (SC-cuts); upper turning point range (AT-cuts).
[b] Calibration at turning point.
[c] See Section 3.7 for definition.

the pole-zero spacing of the corresponding AT; this increased *stiffness* means greater stability for a given overtone. The multiplicity of modes makes the circuit design more difficult for SCs, but the fact that these resonators are compensated against frequency changes caused by electrode stresses (a large component of long-term aging in ATs) and compensated against thermal transient effects (a contributor to short-term instabilities in ATs) more than makes up for these inconveniences for high-stability applications.

3.4 SURFACE ACOUSTIC WAVE (SAW) DEVICES[3.16, 3.19]

The waves considered in prior sections are called bulk acoustic waves (BAWs) because they travel within the bulk of the resonator and are reflected at the surfaces to form standing waves at resonance. Another species of wave motion exists and is called a surface acoustic wave (SAW). As its name implies, the motion is concentrated at the surface of the crystal; the wave motion decays exponentially with distance from the surface, so that typically 90 to 95% of the energy is contained within one acoustic wavelength of the surface. Corresponding to the BAW AT quartz cut is the SAW ST-cut. This is a singly rotated cut with $\theta \approx +42°$ to 43°, and has favorable frequency–temperature behavior (see Section 3.7).

Excitation of SAWs piezoelectrically is accomplished by means of interdigital transducers (IDTs). These are a series of electrode stripes of alternating polarity, shown schematically[3.19] in the center of Fig. 3.18*a*. In practice the stripe widths and the gaps between stripes are equal to one-quarter of an acoustic wavelength at resonance. In AT and SC BAW resonators the thickness determines the frequency; with IDT patterns the frequency is determined by

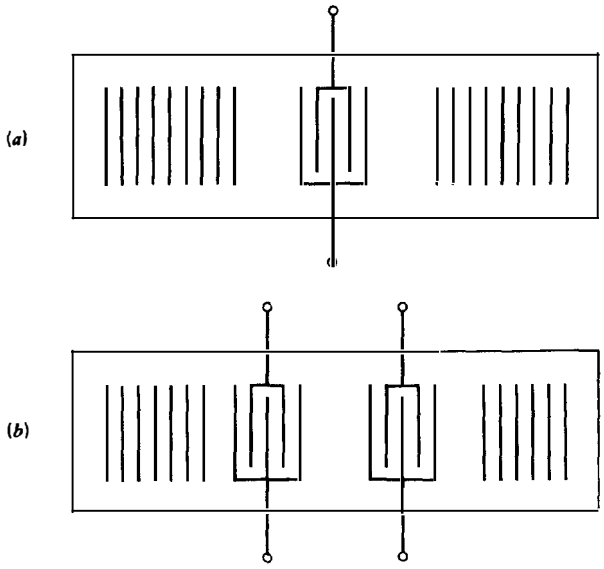

Figure 3.18 (*a*) Schematic representation of a one-port surface acoustic wave resonator (SAWR). Electrode finger spacings, rather than crystal dimensions, determine the resonance frequency. Frequencies well into the GHz region are possible using microelectronic fabrication procedures. (*b*) Schematic representation of a two-port SAWR.

the finger and gap widths. Since these can be made very narrow by photolithographic means, SAW frequencies into the GHz region can be realized on robust substrates.

The earliest SAW devices consisted of two IDT structures separated by hundreds of wavelengths, thus forming an acoustic delay line. These two-port devices were then used as filters by adjusting the IDT finger lengths and separations. Delay-line oscillators were also used, but the circuit element of greatest interest in oscillator design is the SAW resonator (SAWR). Figure 3.18 shows both one- and two-port varieties. The unconnected fingers that appear at the ends of the SAWRs are reflectors that may be either deposited metallic fingers or etched grooves. Either structure presents a slight acoustic discontinuity to the waves, which when summed over many hundreds of reflectors, returns almost all of the energy to the central *cavity* and produces a high Q_x value. Aluminum is the electrode material preferred for SAW application with quartz because its acoustic impedance is within a few percent of that of quartz. At a high power level it has been observed that the electric fields produced near the finger edges tend to make the aluminum migrate, to the detriment of the aging and device properties; doping the aluminum with copper greatly reduces the effect.[3.21]

The device in Fig. 3.18*a* has exactly the same equivalent circuit as that of a BAW resonator, namely, that of Fig. 3.5. The circuit values are functions of the number and spacing of the IDT and reflector fingers and of the material

Table 3.7 Parameter Values for ST-Cut Quartz One-Port Surface Wave Resonators[3.19]

f (MHz)	C_0 (pF)	R_1 (Ω)	r (10^3)	C_1 (10^{-3} pF)	Q (10^3)	M	$\Delta f/f^a$ (10^{-6})
50	10	25	11.8	0.85	150	12.7	± 15
50	20	50	25.1	0.80	80	3.2	± 15
500	2	20	2.5	0.80	20	7.9	± 15
500	4	50	7.5	0.53	12	1.6	± 15
1000	1	100	6.3	0.16	10	1.6	± 15
1000	2	250	25.1	0.080	8	0.32	± 15

[a] Frequency tolerance over temperature range 0°– + 55°C.

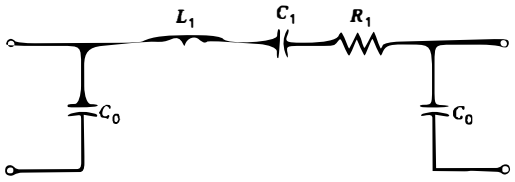

Figure 3.19 Equivalent circuit of the two-port SAWR. Because C_0 does not shunt the motional arm, this device is preferred in many applications over the one-port SAWR, whose equivalent circuit is that shown in Fig. 3.5.

constants of the substrate crystal. Representative values[3.19] are given in Table 3.7.

A two-port SAWR[3.19] is shown in Fig. 3.18*b* and represented by the circuit of Fig. 3.19. Because the C_0 does not shunt the motional arm as it does with Fig. 3.5, compensation of C_0 by a shunt inductor is not necessary with this device. Element values from Table 3.7 are representative for the motional arm. In both types of SAWRs, the R_1 value is very temperature dependent and must be carefully regarded in practical designs. The frequency tolerance given is for the temperature range 0 to 55°C.

3.5 MINIATURE RESONATORS

In the design of most kinds of traditional resonators, the emphasis is placed on obtaining as uncomplicated a type of vibratory motion as possible, for example, pure thickness shear, or flexure. In some cases coupled motions are employed, as in GT- and SL-cuts, but even here the pattern of the motion is not too complicated. Most recently, driven by the need to obtain resonators of small size for wristwatches, much effort has been placed on the analysis and design of units that employ more complicated coupled motions, for example, coupled thickness shear and flexure together. The coupling affords the possibil-

Table 3.8 Representative Parameters for Miniature Quartz Resonators

Shape	Vibration Type	f Range (kHz)	C_0 (pF)	R_1 (Ω)	C_1 (10^{-3} pF)	Q (10^3)	XYZ Dimensions (mm)	Temperature Coefficient	Ref.
Fork	Overtone flexure	10–1000		10k–40k	0.4–2.5	80–250	1.0 × 2.6 × 0.13	$a_0 = 0$; $b_0 = -30$	3.22
Rod	Length extension	1000		2.5k/600	0.3/1.3	200	0.9 × 3.4 × 0.10	$a_0 = 0, b_0 = -40$	3.23
Bevelled rectangle	DT Contour shear	500–1000			14–4.5		40 × 0.8 × 3.0		3.24
Rectangular plate	Edge	712.6/1180	0.13/0.080	40k	0.13/0.086	40	15.2 × 3.2 × 0.8 9.5 × 2.0 × 0.5	$a_0 = 0, b_0 = -39$ to -64	3.25
Cylindrical strip	AT shear	4194	1.35	53.9	3.45	223	6.0 × 0.4 × 1.6	$a_0 < \pm 0.06$	3.26
Rectangular plate	GT coupled extension	2300		110	2.5	200–300	1.41 × 1.47 × 0.07	$a_0 = b_0 = 0$; $c_0 = 4.5$	3.27
Fork	Flexure	200	1.0	3k	1.0	300	0.9 × 2.9 × 0.16	$a_0 = 0$; $b_0 = -15, -30$	3.28
Fork	Flexure	100 (50–200)	1.0	10k	1.0	200	0.9 × 4.7 × 0.10	$a_0 = 0$; $b_0 = -10, -20$	3.29
Rectangular plate	Width extension	1049			1.2	200–300	2.7 × 4.0 × 0.20	$a_0 = b_0 = 0$; $c_0 = +50$	3.30
Fork	NT flexure	32.768	1.05	28k	1.76	> 60	1.1 × 4.7 × 0.10		3.31

Table 3.9 Typical Parameter Values for Thin-Membrane Plate Resonators of Quartz and Lithium Tantalate

Cut	N	f (MHz)	C_0 (pF)	R_1 (ohms)	r (10^3)	C_1 (10^{-3} pF)	Q (10^3)	M	C_{d_1} (pF)
AT	3	450	0.6	250	10.7	0.056	24	2.24	0.4
BT	3	465	0.7	116	18.4	0.038	76	4.13	0.8
AT	1	100	1.34	30	1.8	0.74	67	37.2	
AT	3	450	1.83	250	30.	0.061	24	0.80	
AT	5	500	1.27	550	60.	0.021	25	0.42	
BT	1	575	1.25	20	3.0	0.42	30	10	
BT	3	470	1.69	90	35.	0.048	80	2.29	
BT	5	475	1.65	420	70.	0.024	36	0.51	
$LiTaO_3$	1	240	1.58	150	0.10	15.8	0.30	3.00	
$LiTaO_3$	3	720	1.90	150	0.75	2.53	0.75	1.00	

ity of obtaining good temperature behavior along with useful motional parameters.

Many of the miniature resonators employ novel support structures that are part of the resonator design. Most are produced by mass-production techniques employed by the microelectronics industry, such as photolithography. The units are sized to fit into tubular watch crystal enclosures (2 mm diameter, 6 mm length) or tiny ceramic packages (1.5 × 2.4 × 6.7 mm).

Table 3.8 contains parameter values on a representative set of miniature resonators. The next-to-last column lists the temperature coefficients (see Section 3.7). The units are a_0 in $10^{-6}/°C$, b_0 in $10^{-9}/°C^2$, and c_0 in $10^{-12}/°C^3$.

In the category of miniature resonators are the thin-membrane plate vibrators.[3.32] These are ordinary crystal plates that have had the material in the central part of the plate removed by ion or chemical milling to form a thin membrane that is supported along its periphery. The membrane vibrates in thickness shear like a conventional plate vibrator. Table 3.9 lists parameter values for AT- and BT-cut quartz and for lithium tantalate membranes.[3.33] The equivalent circuit for the first two entries is that of Fig. 3.4 with $C_{d_1} = C_{d_2}$.

3.6 UNDESIRED RESPONSES

Finite crystal plates in general have a complicated mode spectrum. One often strives to have a simple distribution of motion and as little coupling as possible and so obtain a clean spectrum. Recipes for the design of AT and BT plate resonators have been worked out that minimize the presence of undesired responses; these criteria are known as *energy trapping* rules.[3.34] These rules require a relationship between the electrode and plate geometry to be satisfied. If a plate resonator is designed without trapping, then the resulting spectrum

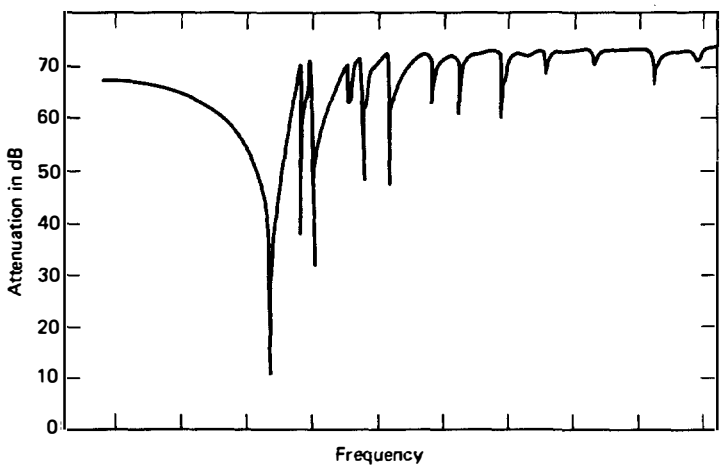

Figure 3.20 Mode spectrograph of a plate resonator. The unwanted modes placed above the main resonance make this unit unfit for filter application, but the 20-dB suppression of the strongest unwanted mode is usually sufficient to guarantee proper operation in an oscillator. Specifying units suitable for filters in oscillator applications would result in greatly increased cost.

will appear like that in Fig. 3.20; often the responses above the main, desired mode will be as strong, or stronger, than the main mode. If the unwanted responses are 10 dB, or more, weaker than the main response, then for oscillator applications the unit is generally acceptable. Certain obscure effects are dealt with in Chapter 18 where the unwanted modes pose a problem. Otherwise, such responses need to be minimized only for filter application. For use in oscillators the required amount of unwanted mode suppression may be simply obtained by contouring[3.35] or bevelling the plate edges and by keeping the ratio $D/D_e > 2.5$, as is the case in the illustrative example in Section 3.2.4.3. The equivalent circuit for the unwanted modes is that of Fig. 3.16*a*, but with much more complicated relations between the parameters of the motional arms than Eqs. (3.40), (3.41), and (3.42).

3.7 STATIC TEMPERATURE EFFECTS

When temperature is slowly varied it is found that the frequency shift due to the variation can be expressed in the form:

$$\frac{\Delta f}{f} = a_0(T - T_0) + b_0(T - T_0)^2 + c_0(T - T_0)^3 \qquad (3.47)$$

T is the temperature variable and T_0 is a reference temperature, often taken as 25°C. The coefficients a_0, b_0, and c_0 are the first-, second-, and third-order

Table 3.10 Higher-Order Temperature Coefficients of Quartz Cuts

	b_0 $(10^{-9}/°C^2)$	c_0 $(10^{-12}/°C^3)$
AT	0.4	110
BT	−40	−128
SC[a]	−12.3	58.2
ST	−34	
CT	−57	−161
DT	−19	75
5°X	−25	
GT	0.2	−26

[a] c mode; for mode b, $a_0 \approx -26 \times 10^{-6}/°C$.

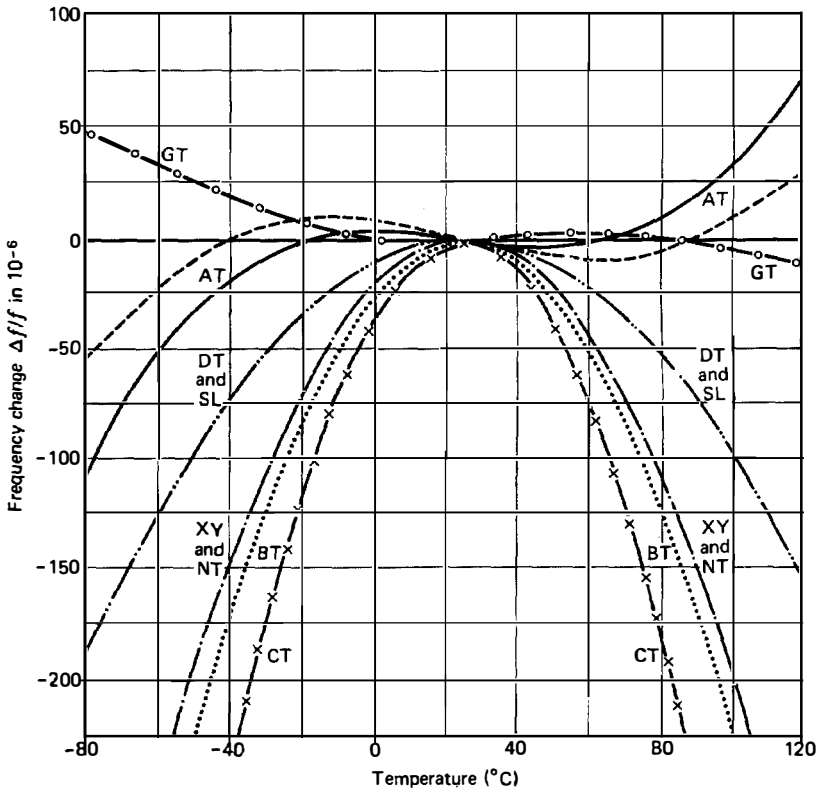

Figure 3.21 Frequency–temperature characteristics of quartz cuts when temperature is changed slowly. The curves may be shifted by small changes in orientation angles.

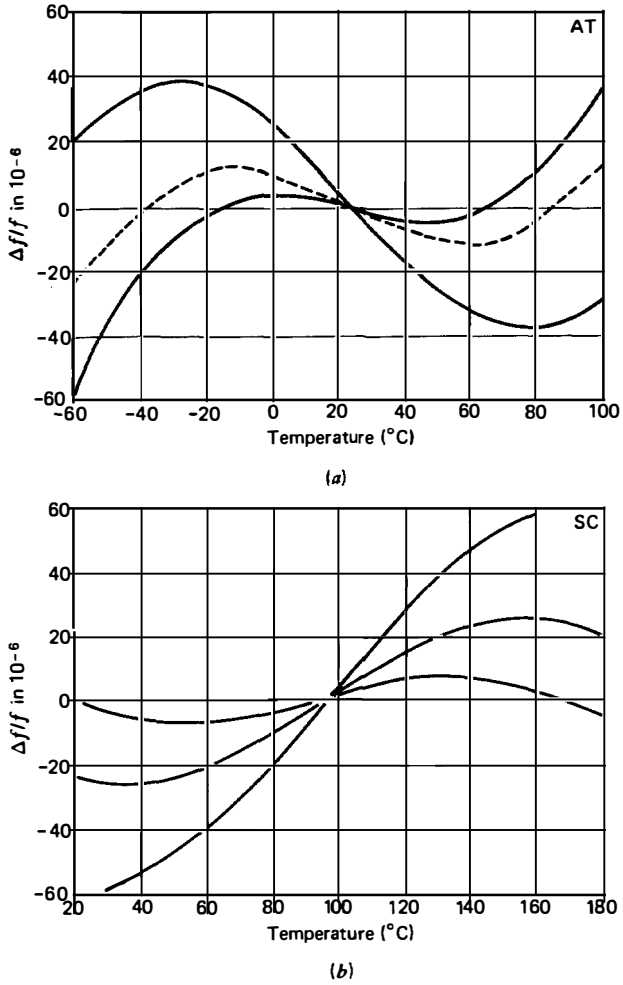

Figure 3.22 (*a*) Static frequency–temperature curves for members of the AT-cut family. Changes in angle θ produce the changes in maximum and minimum points permitting an orientation to be found that minimizes frequency change over a specified temperature range. The dotted curve is the *optimum* AT-cut, with variation of only ± 12 ppm from $-50°$ to $+100°$C. (*b*) Static frequency–temperature curves for members of the SC-cut family. The inflection temperature is approximately 96°C.

temperature coefficients of frequency, and are usually expressed in units of $10^{-6}/°C$, $10^{-9}/°C^2$, and $10^{-12}/°C^3$, respectively. The temperature coefficients a_0, b_0, and c_0 and the thickness modes *a*, *b*, and *c* share a somewhat common notation that arose for historical reasons, but no confusion should arise. The cuts of interest for oscillator application are those having either zero or small a_0 values, and reasonably small b_0 and c_0 values. Some examples occur in the next-to-last column of Table 3.8.

If T_0 is taken where the frequency–temperature (f–T) slope is zero, then $a_0 = 0$, and the curves are determined by the b_0 and c_0 values. Table 3.10 lists values, for a number of quartz cuts, of the quantities b_0 and c_0.[3.37] Frequency–temperature graphs are given in Figs. 3.21 and 3.22.

When T_0 is taken such that b_0 is zero, the temperature is referred to as the inflection temperature T_i; an example appears in the last column of Table 3.6. The inflection temperature has been used for T_0 in Fig. 3.22. In both parts of this figure is seen the effect on the cubic curve of changes in the angle θ. By adjustment of θ during manufacture the f–T curve may be controlled to provide the minimum frequency excursion over a specified operating temperature range. The normal low and high limits on the f–T curves are shown in the figure for the AT and SC families of cuts. Changes in orientation angle provide means to adjust the cuts having parabolic curves in Fig. 3.21; the turn-over temperature can be moved 20 or 30°C for special applications. The dashed curve in Fig. 3.22*a* shows the *optimum* AT-cut, which has the least frequency change (about ±12 parts per million) over the range −50 to +100°C.

Figure 3.23 relates the frequency tolerance, for AT-cuts, to be expected in manufacture when the angle tolerance $\Delta\theta$ is specified. The curve labeled A covers the temperature range −55 to +105°C. If an angle tolerance $\Delta\theta$ due to x-raying, lapping, polishing, and so on, is known for a particular product line, say ±3 min of arc, and if the desired operating range is that specified by A, then the frequency tolerance of the finished units will be within ±30 ppm over that temperature range. Tightening the angular tolerance to ±1 min of arc will

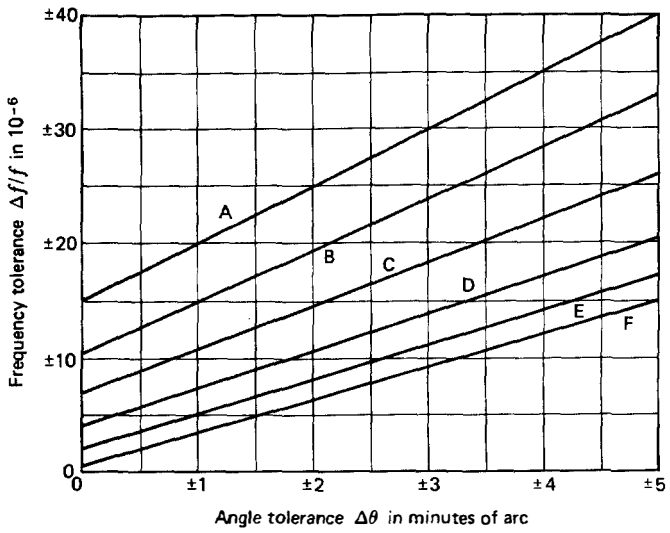

Figure 3.23 Frequency tolerance obtained with units manufactured with a specified angle tolerance $\Delta\theta$. The curves indicate the operating temperature range in °C as follows: A = −55 to +105; B = −45 to +95; C = −35 to +85; D = −25 to +75; E = −15 to +65; F = −5 to +55.

reduce the $\Delta f/f$ tolerance to ± 15 ppm. The practical consequences of this graph are obvious. Specifying a certain frequency tolerance that is too tight and/or specifying an operating temperature range that is too broad will require units that are costly to produce.

By means of Eqs. (3.16) and (3.36) one may show that the difference in the slopes of the $f-T$ curves of a resonator operated at f_R and at f_L depends upon the temperature coefficient of the piezoelectric coupling factor k. This effect is non-negligible for quartz and must be taken into account in the design of TCXOs.[3.36]

3.8 AGING EFFECTS

Slow changes in frequency with time are referred to as resonator aging. The principal causes of aging are contamination within the enclosure that is redistributed with time, slow leaks in the enclosure, mounting and electrode stresses that are relieved with time, and *oilcanning*, where the enclosure is stressed by changes in atmospheric pressure outside the envelope. Changes in the quartz are usually negligible for most applications.

A typical aging curve is given in Fig. 3.24.[3.38] The curve marked A ages upward in frequency in approximately logarithmic fashion. The positive aging

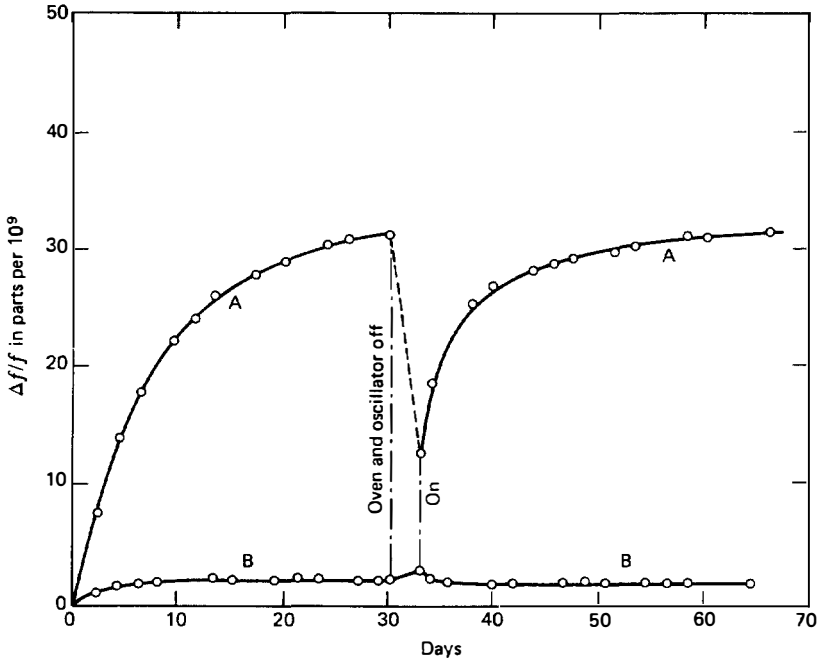

Figure 3.24 Frequency changes in precision quartz crystal units due to interruptions in oscillation and oven control. A: solder bonding and glass encapsulation. B: thermocompression bonding and high-temperature processing.

shown is the most common form; it might arise from contamination on the vibrator surfaces during inoperation being redistributed to the other portions of the enclosure when the crystal is in motion.[3.39] This is seen to be probable from the response to turn-off and subsequent restart. The cleaner crystal of curve B has a much reduced aging. Negative aging is usually caused by enclosure leakage.

Aging is also a function of drive level of the crystal unless contamination and stresses have been minimized by use of high-temperature high-vacuum bakeout and sealing and use of SC-cuts.

In high-volume production aging rates less than 1 part in 10^8 per day can be achieved; for high-precision units the figure can be improved to 5 parts in 10^{11} per day on a low-yield selective basis.

3.9 ENVIRONMENTAL EFFECTS (EXCLUDING STATIC TEMPERATURE EFFECTS)

Figure 3.25 shows an idealized curve of frequency versus time for a crystal resonator subjected to a variety of environmental disturbances.[3.40] A thermal transient occurs at t_1; mechanical accelerations in the forms of vibration, shock, and turning the crystal over in a gravitational field (tip-over) occur between t_2 and t_7. At t_5 the oscillator is turned off, causing another thermal transient, and at t_6 it is turned back on again. Superimposed on these disturbances is the long-term aging slope discussed briefly in Section 3.8. If the curve is sufficiently magnified, it will be found to contain noisy fluctuations (see Section 3.13) about the mean frequency.

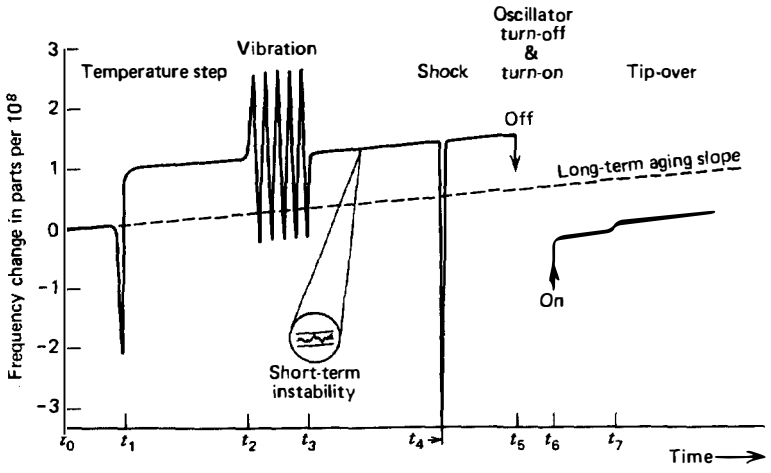

Figure 3.25 Idealized frequency–time behavior of a quartz oscillator. The greatest contributors to frequency change are thermal transients, accelerations, cessation, and reestablishment of vibration, and long-term aging.

3.9.1 Thermal Transients[3.43-3.45]

The f–T curves in Section 3.7 assumed slow temperature variations. If $dT/dt = \dot{T}$ is sufficiently large to produce thermal gradients across the resonator, then it is found that the curve of Eq. (3.47) must be modified to read

$$\frac{\Delta f}{f} = a_0 \Delta T + b_0 \Delta T^2 + c_0 \Delta T^3 + (\tilde{a}\,\Delta T + \hat{a})\dot{T} \tag{3.48}$$

where $\Delta T = \Delta T(t) = T(t) - T_0$. In Eq. (3.48), $\tilde{a}$ and $\hat{a}$ depend upon material constants of quartz as well as the resonator design. For tests involving a ramp function of temperature, the $\tilde{a}$ coefficient has the effect of changing the apparent angle of orientation of the resonators; that is, it rotates the S-shaped cubic curve. The $\hat{a}$ coefficient translates the cubic curve up or down in frequency. When an abrupt temperature change is encountered, as with oven turn-on, AT-cuts will behave as seen in Fig. 3.26, producing an overshoot and slow approach to equilibrium.[3.41] SC-cuts, on the other hand, experience no such transients and simply follow the static f–T curve irrespective of $\dot{T}$.

The consequences of this difference in behavior are striking when one has to adjust the oven of a high-precision unit to the turnover (zero-slope) point of the f–T curve. Even minute changes in temperature will send the AT-cut oscillator's frequency far from where the static curve would predict, and many oven time constants have to be waited for the frequency to settle finally at the

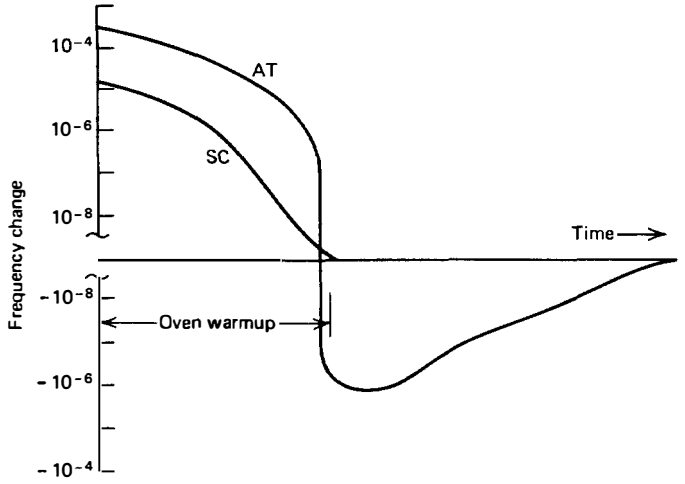

Figure 3.26 Response of AT- and SC-cuts to a thermal transient, due to oven warmup. Thermal gradients in the AT produce a dramatic overshoot and a long approach to steady state; the thermally compensated SC approaches final frequency in a time dictated solely by the oven parameters.

static point. Creeping up on the turn-over temperature in this manner is exceedingly time-consuming and costly.

Moreover, when the oven has been set at its reference point, it can only maintain the temperature within a finite range. If this range is used in Eq. (3.47), the $\Delta f/f$ so predicted will be found to be many times smaller than that observed. The $\tilde{a}$ and $\hat{a}$ terms can cause substantial frequency departures in high-precision AT oscillators.

In SC-cut resonators the effect is nearly absent, and the setting the oven temperature to the turn-over point is a simple rapid procedure.

3.9.2 Thermal–Frequency Hysteresis[3.42]

Figure 3.27 gives an example of thermal hysteresis encountered when cycling a quartz resonator over an extended temperature range. The effect is a function of the temperature range; its causes are poorly understood. It should be borne in mind that the effect varies from unit to unit and is very difficult to model for the purpose of compensation by microprocessor programming.

3.9.3 Acceleration Effects

Shock, vibration, and change in attitude (tip-over) are acceleration effects. For a given design and direction of applied acceleration, the frequency shift is

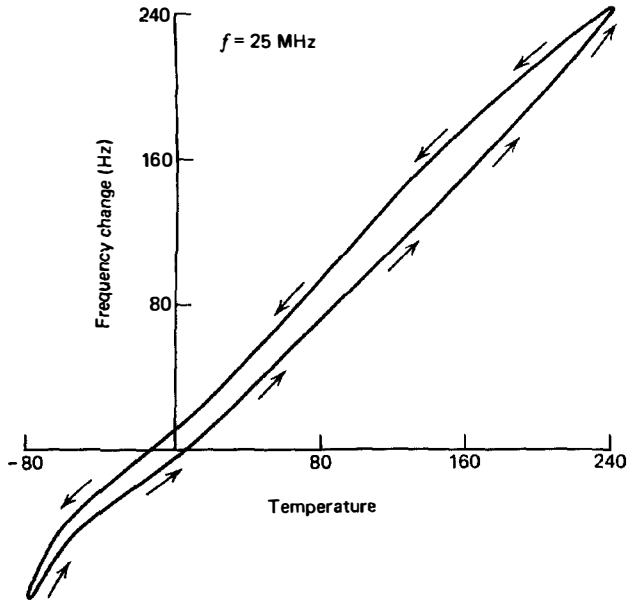

Figure 3.27 Thermal hysteresis in quartz resonators. Cycling over wide temperature extremes produces hysteretic behavior that approaches a semireproducible loop after a number of repetitions; changing the temperature excursions modifies the loop.

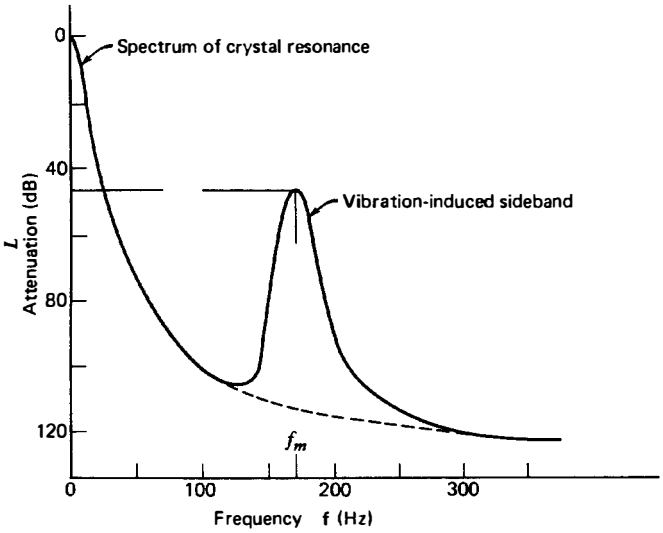

Figure 3.28 Crystal resonance spectrum showing vibration-induced sideband at modulation frequency f_m. Sideband level, referred to the crystal resonance, is a measure of the crystal's acceleration sensitivity.

proportional to the acceleration $\bar{a}$:

$$\frac{\Delta f}{f} = \bar{a}\gamma \tag{3.49}$$

$\bar{a}$ is expressed in g units and γ is the acceleration sensitivity coefficient. Values for γ normally run a few parts in 10^9 per g for the AT-cut. Recent work has led to units with γ values in the 10^{-10} range, but with relatively labor-intense methods.

If a resonator operating at its resonance frequency is subjected to a sinusoidal vibration at frequency f_m, where $f_m \ll f_R$, then sidebands will be produced at the carrier frequency $\pm f_m$. An example is shown in Fig. 3.28. A measurement of the sideband level L, in dB, normalized to the carrier level, determines γ from

$$\gamma = \left(\frac{2f_m}{\bar{a}f}\right) \times 10^{L/20} \tag{3.50}$$

3.9.4 The Polarization Effect

A dc voltage impressed on the electrodes of an AT-cut will produce a very small frequency shift; for an SC-cut the effect is considerably larger and may be utilized for compensation purposes. Expressed in terms of a constant $\bar{e}$, we

obtain

$$\frac{\Delta f}{f} = \bar{e}E \tag{3.51}$$

E is the vacuum electric field strength. For AT-cuts, $\bar{e} = 0.04$ and for SC-cuts, $\bar{e} = 2.3$; the units of $\bar{e}$ are 10^{-9} mm/V, and of E are V/mm. If 10 V dc is applied to a typical 5-MHz fundamental SC-cut, the normalized frequency shift is approximately 6×10^{-8}. In some circuits static electricity can accumulate across the crystal terminals, leading to a frequency shift caused by the polarization effect. If this charge fluctuates with time, an added contribution to noise will then be present (see Section 3.13). By shunting the crystal by a high resistance, this influence can be overcome.

3.10 DRIVE LEVEL EFFECTS

The apparent resistance of a resonator is often found to be a function of the crystal current I_x. The effect is sketched in Fig. 3.29. The motional capacitance C_1 may also vary with drive, but its variation is much less than that of R_1.

3.10.1 Second Level of Drive[3.43, 3.48]

At low drive levels, the resistance R_1 of many crystals increases appreciably, and very often abruptly. Examples are given in Figs. 3.30*a* and 3.30*b*. In Fig. 3.30*a*, as the voltage across the crystal is increased from 0 to B, the current

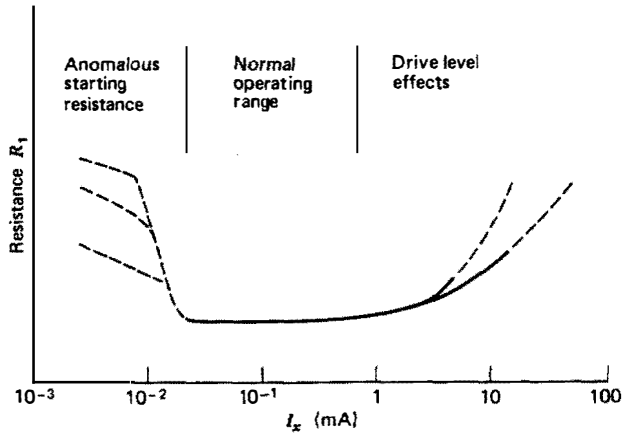

Figure 3.29 Schematic representation of the variation of resonator motional resistance with crystal current. At very low values anomalously high resistances are sometimes encountered; at high drive levels nonlinear effects increase the resistance.

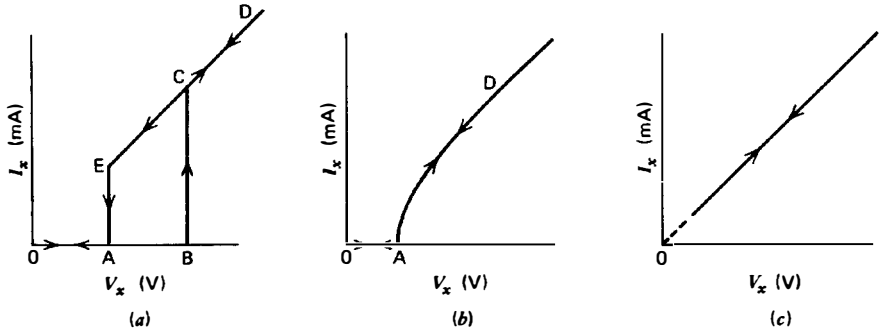

Figure 3.30 (*a*) Anomalous starting resistance occurring as abrupt transitions leading to a hysteresis loop. (*b*) Nonlinear starting resistance occurring as a single-valued function of crystal voltage V_x. (*c*) Normal linear crystal resistance extending down to very low values of V_x.

remains zero. It rises abruptly to point C, where its value is consistent with the rated R_1. Further increases in V_x produce no change in R_1, nor do decreases until point E is reached when I_x again falls to zero. The hysteresis-like effect is called *second level of drive*.[3.46] In some resonator units the behavior shown in Fig. 3.30*b* is encountered where the curve shows a continuous increase in R_1 with decrease in V_x from point D to point A, and no crystal activity for V_x values below this.

This effect is almost exclusively due to the surface preparation of the resonator. It becomes apparent at current densities below about 10 μA/mm^2, which, for units in HC-6 and HC-18 enclosures, and for frequencies in the 1–30-MHz range, works out to mA currents and μW power levels.

It is obvious that the presence of this effect can produce serious starting and operating effects in the oscillator. Furthermore, the effect can be insidious and not show up in tests on a newly made resonator, only to appear after a period of storage.

Production of units without this defect requires attention to surface cleanliness. Maintaining the resonator surface free from contaminating particles of lapping and polishing compound and use of chemical etching to remove microcracks effectively removes the phenomenon and results in units with the characteristic shown in Fig. 3.30*c*. The effect is thought to be much less severe with SC-cuts than with AT. It may be dealt with in the specification of the unit.

3.10.2 Amplitude–Frequency Effect[3.49,3.50]

At higher levels of drive the resonance curve ceases to be symmetric and bends to one side as shown in Fig. 3.31.[3.47] The AT-cut behaves as a *hard spring* and bends toward higher frequencies; the BT-cut acts like a *soft spring* and bends toward lower frequencies. The locus of the maxima of the resonances is given

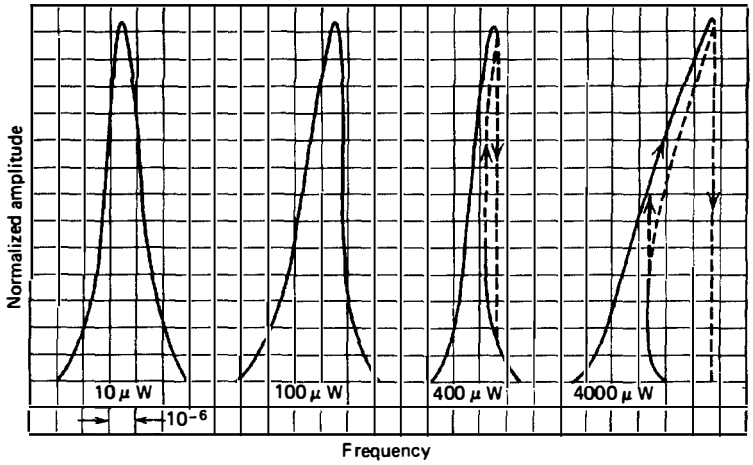

(*a*)

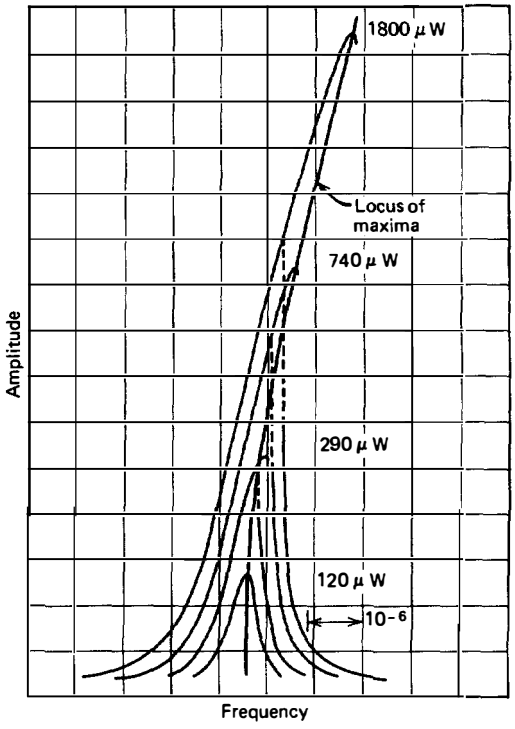

(*b*)

Figure 3.31 (*a*) Amplitude–frequency effect. As drive level is increased the crystal resonance curve becomes a multiple-valued function of frequency. Curve heights have been scaled to the same value. (*b*) Amplitude–frequency curves superimposed, showing the locus of maxima. The resonator is an AT-cut at 1 MHz.

by

$$\Delta f/f = aI_x^2. \tag{3.52}$$

For conventional AT designs at 5 and 100 MHz, a is approximately 0.20 to $0.25/A^2$. Values of a between $0.02/A^2$ and $0.05/A^2$ have been reported,[3.49, 3.50] for doubly rotated cuts, with ϕ angles in the range $\pm 2°$ of the SC-cut, at both third and fifth overtones. With planoconvex designs, a decreases with decreasing curvature and is smallest in flat plates. The effect depends upon geometrical design, material, overtone, and mode of motion. The lowest a value measured to date on a BAW resonator is $0.004/A^2$ on a third overtone, doubly rotated plate having $\phi = 20°$. ST-cut SAW devices have even lower values; a value of $a = 0.0011/A^2$ at 110 MHz has been measured.

The amplitude–frequency effect is more correctly characterized by use of current density rather than I_x in Eq. (3.52); when put on this basis the effect becomes perceptible at densities of roughly 50 $\mu A/mm^2$ for AT-cuts. Since in most designs electrode area decreases with increasing frequency, keeping I_x constant for units of increasing frequency would mean increasing the current density. In order to keep the maximum frequency change $\Delta f/f$ constant, I_x should therefore decrease in higher-frequency units.

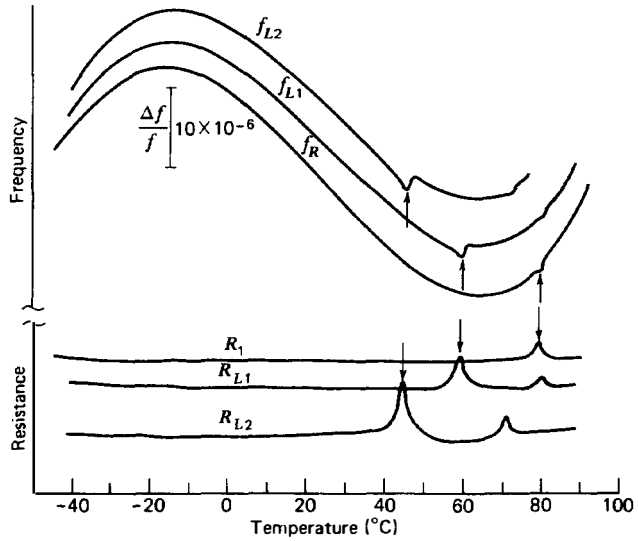

Figure 3.32 Activity dips in the frequency–temperature plots of an AT-cut when operated without and with load capacitors. Crystal parameters: $f = 20$ MHz; $C_0 = 2.1$ pF; $R_1 = 3\ \Omega$; $C_{L1} = 35$ pF; $C_{L2} = 22$ pF; $I_x = 2$ mA. All curves have been vertically displaced for clarity. The activity dip temperature is a function of C_L indicating that the dip is caused by coupling to a flexure mode with a large negative temperature coefficient.

3.11 ACTIVITY DIPS[3.51, 3.70]

An example of an activity dip in the $f-T$ curve of an AT resonator is shown in Fig. 3.32. It appears in both the frequency and in the apparent crystal resistance. It is a potential source of difficulty for oscillator applications and is dealt with in the specification of the unit. No activity dips have yet been observed in SC-cuts.

Slow changes in R_1 with temperature are often encountered; these are not activity dips. In the resonator specification the maximum value of resistance over the temperature range should be specified, not simply the resistance at a reference temperature. In oscillators that are operated over a range of temperatures, changes in crystal resistance with temperature will produce drive level output power changes.

3.12 RADIATION EFFECTS[3.52-3.55]

Two types of resonator radiation effects are usually distinguished: (1) collision processes due to neutrons and α-particles, and (2) ionizing radiation effects due to x-rays, gamma rays, and electrons.

3.12.1 Neutrons

Displacement damage produces permanent frequency shifts in quartz resonators because it modifies the effective elastic constants. Since the effect is very structure sensitive, the type and quality of the quartz material is extremely important. Permanent displacement damage due to neutrons shifts the resonator frequency at the approximate rate $\Delta f/f \approx 10^{-21}/\text{cm}^2/\text{neutron}$.

3.12.2 Ionizing Radiation

Most resonator radiation sensitivity work has been done in this area. The ionizing radiation effect depends upon (1) the amount of impurities present in the quartz and (2) upon the temperature profile created. Aluminum often substitutes for silicon in quartz, where a proton, or ion of lithium, sodium, or potassium compensates for the additionally needed charge. The radiation makes the monovalent ions migrate along the relatively open Z-axis channels within the quartz, and produces frequency changes.

Pulsed ionizing radiation produces frequency changes in quartz resonators, even in the absence of impurities, because thermal gradients are set up in the quartz, leading to changes in the nonlinear elastic constants. The effect depends on the crystal cut, being negative for the AT-cut, but is almost insensitive to the type (natural or cultured) of quartz used, and to the quality, although Q degradation and even cessation of the oscillation has been observed when impure quartz is used. Temperature gradient effects on resonator

frequency, arising from pulsed ionizing radiation, can be largely compensated by utilizing SC-cut resonators. These will, however, still be subject to frequency shifts due to impurities, if present.

Steady-state radiation effects depend strongly on defects in the material. Just as annealing has been used to increase the Q of quartz, a combination of high temperatures (from 350 to 550°C) and strong electric fields (referred to as *sweeping*) has been found to produce material with superior purity and thus superior radiation hardness. Swept Z-growth cultured quartz is the most radiation tolerant; this is a consequence of the removal of sodium, lithium, and potassium ions. The sweeping process (done in a vacuum) has also been shown to produce material having fewer etch channels than nonswept cultured quartz. Etch channels degrade the strength (shock resistance) and serve as repositories of etchant that can produce long-term aging.

Typical values for the frequency change due to ionizing radiation are

$$\frac{\Delta f}{f} \approx \begin{cases} \text{natural quartz: } 10^{-11}/\text{rad} \\ \text{swept cultured quartz: } < 10^{-12}/\text{rad} \end{cases}$$

3.13 NOISE IN QUARTZ CRYSTALS[3.43, 3.44, 3.57, 3.59]

This topic is just beginning to receive the attentions of researchers to the extent it deserves. For some years it has been known that one source of noise arising from the crystal itself is the thermal noise associated with its temperature of operation. The equivalent noise resistance of a quartz crystal is the same as its effective series resistance R_1 at the using temperature. This leads to a noise voltage of[3.57]

$$v(\text{noise}) = \sqrt{4k_B TB} \tag{3.53}$$

where $k_B T$ is 5×10^{-21} W-s at room temperature, and B is the bandwidth in which the voltage is measured. The crystal can be considered at resonance to be a narrowband filter for the additive wideband noise voltage of Eq. (3.53).

In addition to this noise source, it is suspected that stress relaxation in the electrodes, as well as correlations with vibrations, via the coefficient γ [see Eq. (3.49)], and correlations with temperature fluctuations via the coefficients $\tilde{a}$ and $\hat{a}$ [see Eq. (3.48)] are operative to produce noise effects. An oven improvement can lead to considerably better noise performance when using resonators with non-negligible $\tilde{a}$ values.[3.60]

The short-term stability is mostly limited by the thermal noise and can be improved by increasing the crystal drive; however, the circuit noise is usually very much greater than the crystal noise unless one deliberately overdrives the resonator. If the crystal drive level is too high, however, the flicker (f^{-1}) noise and the higher-order noise components ($f^{-2}, f^{-3}, f^{-4}, f^{-5}, \ldots$) all become

much higher; this includes the amplitude-to-frequency noise conversion via the coefficient a [see Eq. (3.52)].

Static charges may build up across the resonator in certain circuit configurations, and if these fluctuate, an additional contribution to noise will be produced; a high shunting resistance will prevent this (see Section 3.9.4).

3.14 GENERAL SPECIFICATIONS

A specification is a set of basic ordering information. The simplest such set for crystal resonators might consist of only three numbers: holder type, nominal frequency, and C_L. Such a specification, or *spec*, would be appropriate only for the least-accurate applications. For the resonators required for the designs contained in this book, it is necessary to specify explicitly the crystal parameters mentioned as inputs in the design algorithms. These are the cut, overtone, R_L, C_L, C_1, and C_0.

In addition to the above, several other important characteristics are in general called for; a representative list might be as follows:

Description

1 Type of crystal enclosure.
2 Nominal frequency.
3 Overtone order, N.
4 Marking.

Operating Circuit Conditions

1 Crystal enclosure grounded or not.
2 Load capacitance C_L.
3 Level of drive.
4 Reference temperature.
5 Operating temperature range.

Frequency Tolerance

1 Overall tolerance.
2 Adjustment tolerance and tolerance over the temperature range.

Electrical Characteristics

1 Parallel capacitance C_0.
2 Motional capacitance C_1.

3 Rated resistance at C_L, R_L.
4 Insulation resistance.
5 Effect of drive level.
6 Unwanted responses.
7 Aging.
8 Permissible deviation of frequency from a smooth function over the operating temperature range.
9 Permissible deviation of resistance from a smooth function over the operating temperature range.
10 Absence of high starting resistance effects.

Mechanical and Climatic Characteristics

1 Robustness and tensile strength of terminations.
2 Flexibility of wire terminations.
3 Bond test of pin terminations.
4 Soldering } Alternatively, an aging specification
5 Sealing } can be given.
6 Vibration.
7 Acceleration.
8 Shock.
9 Operable temperature range.
10 Storage temperature range.
11 Temperature cycling.

There is a general need within the crystal industry today to increase the absolute accuracy of parameter measurements. Because of this, the engineer should fully specify those characteristics that are important in his application. This may include a description of the measurement procedure and possibly specification of an apparatus for the determination of these parameters.

3.15 MILITARY SPECIFICATIONS

Resonators meeting military specifications are required to undergo rigorous inspection and are designed for ruggedness and quality. The user begins with a military standard, or MIL-STD. This is a document for the equipment designer to pick out standard items with desired parameters, but is not used for procurement. It contains only those items recommended for new designs. For crystal units the MIL-STD is given in Ref. 3.61.

Then the user progresses to the military specification, or MIL-SPEC. This is a procurement document for use in purchasing items. It lists parts numbers,

parameters, and tolerances. The crystal specification is given in Ref. 3.62; crystal holders are given in Ref. 3.63.

Finally, one requires a qualified products list, or QPL. This lists those manufacturers qualified to supply the specified items meeting the military requirements.

Crystal resonators are grouped in Federal Supply Classification (FSC) Class 5955: Piezoelectric Crystals.

The agency responsible for military specifications is: Defense Logistics Agency, DESC, Dayton, Ohio 45444. The documents in Refs. 3.61, 3.62, and 3.63 may be obtained through this agency or from Naval Publication and Form Center, 5801 Tabor Ave., Philadelphia, Pa. 19120.

To date, there are no military specifications governing doubly rotated cut BAW resonators (specifically, the SC-cut), SAW resonators, or miniature resonators.

3.16 NATIONAL AND INTERNATIONAL SPECIFICATIONS

The principal nonmilitary sources of crystal resonator specifications and standards in the United States are (1) The IEEE, (2) EIA, and (3) ANSI.

Pertinent IEEE standards are given in Refs. 3.64 and 3.65. They may be obtained from IEEE Service Center, 445 Hoes Lane, Piscataway, N.J. 08854.

The EIA has specifications dealing with holders and sockets, production tests, application information, and cultured quartz. They may be obtained from Electronic Industries Association, 2001 Eye St., NW, Washington, D.C. 20006.

ANSI interfaces with international standards groups such as the International Electrotechnical Commission (IEC). Typical IEC publications are given in Refs. 3.66, 3.67, and 3.68. These IEC documents may be obtained in the United States from American National Standards Institute, 1430 Broadway, New York, N.Y. 10018, or directly from International Electrotechnical Commission, 1-3 rue de Varembé, Geneva, Switzerland.

To date, no standards exist to cover doubly rotated cut BAW resonators (specifically the SC-cut), SAW resonators, or miniature resonators.